between transcripts in whole blood and the central nervous system makes it an accessible alternative [45,46]. Several studies utilizing similar strategies to study twin pairs discordant for psychiatric disorders through comparisons of CpG islands methylation of peripheral blood cells or lymphoblast cell lines had detected a number of disease-associated epigenetic changes [47–49]. Moreover, it has been documented that the methylation changes of large-scale domains are linked to cell-specific differentiation [50]. Several functional gene sets we found (i.e., "cation channel activity", "cell-cell signaling", "extracellular region part", "G-protein coupled receptor protein signaling pathway", and "gated channel activity") were observed within neuronal highly methylated domains. The association between expression difference observed in lymphoblast cell lines and neuron-specific methylation patterns implies that these candidate gene sets are more likely to reflect the true differences in brains. Technical limitations of this study include low fold-change differences in expression levels manifested between co-twins. We did not carry out qRT-PCR for the genes identified by GSEA, considering that differences of less than 1.5-fold are thought to be beyond the limit of reproducibility [51].

Reverse causality should be considered in epigenetic studies, considering all known epigenetic marks are influenced by environmental exposures including diet, smoking, alcohol consumption, stress, or physical activities [52], It might be plausible that the changes we observed in this study resulted from the divergent lifestyle choices by subjects with different levels of intelligence, and not that these epigenetic changes caused the twins to differ.

Here, we presented the first study that used genome-wide epigenetic and transcriptomic profiling to identify epigenetic changes related to the discordance between MZ twins with normal-range intelligence. A list of new candidate genes possibly related to cognitive abilities was generated while further replications and functional analysis remain necessary.

## Materials and Methods

### Ethics statement

This study was conducted according to the principles expressed in the Declaration of Helsinki. Attendance was voluntary, and signed informed consent including information on genetic analyses was obtained from all participants. The Ethical Committees of Kobe University Graduate School of Medicine and Keio University Faculty of Letters approved study protocols.

### Samples

A sub-sample of 326 twin pairs of twins from the Keio Twin Project were invited to Keio University, where the Kyodai Nx15-, one of the most often used group intelligence tests in Japan, was applied. The zygosity of participants was diagnosed by 15 polymorphic STR loci (AmpF$\ell$STR identifier kit, Applied Biosystems). Among the 240 pairs to have monozygosity, 34 MZ twin pairs who manifested differences in IQ score of more than 15 points between co-twins. One pair was excluded for a lower-than-normal IQ score (52 points). From the17 of the remaining 33 twin pairs, who agreed to participate in the study, peripheral blood was drawn and B-lymphoblastoid cell lines were established. For the treatment of 5-azadC (WAKO), a daily aliquot of 5 mM stock solution was added to flasks and thoroughly resuspended (final concentration of 1 μM). Cells were harvested after 3 days from the start of treatment.

### Nucleic acids extraction

For human promoter microarrays and bisulfite genomic sequencing, genomic DNA was extracted from the blood via established methods. For gene expression microarrays and quantitative RT-PCR, total RNA was isolated using RNeasy Plus Mini kit (QIAGEN) from B-lymphoblastoid cell lines.

### DNA methylation profiling

One microgram of genomic DNA was sonicated and subjected to methylated DNA enrichment using the MethylMiner methylated DNA enrichment kit (Invitrogen) as per the manufacturer's instructions. The methylated DNA fragments, amplified by the GenomePlex WGA reamplification kit 3 (SIGMA) and supplemented with dUTP, were further purified using the QIAquick PCR purification kit (QIAGEN).

According to Affymetrix's chromatin immunoprecipitation assay protocol, enriched methylated DNA was hybridized to GeneChip Human Promoter 1.0R arrays (Affymetrix), which comprised a coverage of over 25,500 human promoter regions.

AGCC (Affymetrix GeneChip Command Console)-format CEL files were first created, and then converted to GCOS (GeneChip Operating Software, Affymetrix)-format CEL files. For the pairwise analyses, paired CEL files were imported into MAT software to specify candidate regions (approximately 600 base pairs in length) with significantly different probe intensities between co-twins ($p<10^{-6}$).

To detect candidate loci across all 17 twin pairs, we utilized Partek Genomic Suite 6.5 software (Partek) to import the CEL files, and have the data converted to $\log_2$ values after normalized by the RMA (Robust Multichip Averaging) algorithm. After the signal from each probe for the higher-IQ sibling was subtracted from that of the lower-IQ co-twin across all probes, one-class *t*-test with statistical parameters set at $p<10^{-6}$ was carried out to detect significant regions.

### Bisulfite sequencing

Genomic DNA was bisulfite-treated using the Methylcode bisulfite conversion kit (Invitrogen) as per the manufacturer's instructions. Amplification was performed with Takara LA Taq polymerase, with converted DNA-specific primers that were designed using MethPrimer. The amplicons were cloned into vectors using a TOPO TA cloning kit (Invitrogen). We performed direct sequencing of the plasmid DNA that was isolated using PI-200 auto-plasmid-isolator (KURABO) via the ABI 3730xl sequencing system (Applied Biosystems).

### Quantitative RT-PCR

Two micrograms of the total RNA was subjected to reverse transcription using the SuperScript III first-strand synthesis system for RT-PCR (Invitrogen). Gene target amplifications, using Takara SYBR premix Ex Taq, were performed in triplicate in a matter of a serial 10 fold dilution. Housekeeping gene *GAPDH* served as the internal control gene. Mann-Whitney U test was performed to compare the relative expression levels between co-twins.

### Gene expression profiling

We processed 300 nanograms of total RNA using the Ambion WT expression kit and the Affymetrix GeneChip WT terminal labeling kit according to the manufacturers' recommended methods. Hybridization and scanning of GeneChip Human Gene 1.0 ST arrays (Affymetrix), which comprised of more than 28,000 gene-level probe sets, were performed as per the manufacturer's

instructions. Partek Genomic Suite 6.5 software was used to import AGCC-format CEL files and normalize the data according to the RMA algorithm. ANOVA with an FDR-adjusted $p$ set to 0.05 was used to determine those probe sets that were significantly different between the groups of twins with a higher IQ and their lower IQ co-twins. A one-class $t$-test analysis with multiple sample correction was conducted across all $\log_2$ ratios (higher-IQ twin/lower-IQ co-twin) for all 17 twin pairs. We also carried out pair-wise comparison for the expression array data and then included genes with a fold-change value more than 2. Genes replicated in the same tendency (up-regulated in the higher IQ twins, or up-regulated in the lower IQ twins) in most pairs were listed.

In another approach, the twins of each pair were categorized into higher and lower expression groups according to the expression level of every individual gene. A paired $t$-test was carried out to compare the mean IQ scores of the two groups. Corrected $p$ of $10^{-6}$ was applied as the cutoff to define being positive.

GSEA was performed for functionally related genes across a spectrum of gene sets of C2 curated gene sets including BioCarta gene sets (217 gene sets), KEGG gene sets (186 gene sets), and Reactome gene sets (430 gene sets), and C5 GO gene sets (1,454 gene sets) separately. Pre-ranked gene lists, including lists with up-regulated/down-regulated genes in the group of twins with higher IQ scores sorted according to the $p$ calculated by a between-group ANOVA test, and lists for each twin pair with genes sorted by between-sibling fold-change values, were constructed for the analyses. Gene sets with FDR $q$-value<0.25 after 1,000 permutation cycles were considered significantly enriched. Lists of leading edge subset genes, the cores of gene sets that account for the enrichment signal, were then generated. To create the list of enriched genes shared by plural twin pairs, the upper 100 enriched genes of each pair were included in the test.

## Supporting Information

**Dataset S1 Pair-wise comparison of expression array data.** Genes with a fold-change value >2 were included. The positive value of fold-change designates up-regulation in the higher IQ twin, while the negative value designates the other way round. n/a indicates no gene matched the fold-change cutoff value.
(XLS)

**Dataset S2 Pair-wise GSEA results using BioCarta database.** Gene sets with a FDR $q$-value<0.25 were included. n/a indicates no gene set matched the FDR cutoff value.
(XLS)

**Dataset S3 Pair-wise GSEA results using KEGG pathway database.** Gene sets with a FDR $q$-value<0.25 were included. n/a indicates no gene set matched the FDR cutoff value.
(XLS)

**Dataset S4 Pair-wise GSEA results using Reactome database.** Gene sets with a FDR $q$-value<0.25 were included. n/a indicates no gene set matched the FDR cutoff value.
(XLS)

**Dataset S5 Pair-wise GSEA results using GO database.** Gene sets with a FDR $q$-value<0.25 were included. n/a indicates no gene set matched the FDR cutoff value.
(XLS)

**Figure S1 Scatterplot of the 240 MZ twin pairs IQ scores.** This diagram provides an overview of the IQ distribution for all 240 MZ twins from the Keio Twin Study. Each circle identifies one twin pair with its x-coordinate and y-coordinate representing, respectively, the IQ score of Twin A and Twin B. With the black line standing for regression, the correlation coefficient of 0.72 suggests the similarities between twins. Circles located outside of the space between two blue lines indicate twin pairs manifesting between-sibling IQ differences larger than 15 points and were considered to be recruited, while the red arrowhead points to one pair being excluded as a possible subject for a lower-than-normal IQ score.
(TIF)

**Figure S2 Positive correlation between IQ scores differences and the number of loci different in methylation status.** The positive correlation between the number of loci with significant differences in methylation patterns and the differences of IQ scores of the twin pairs was visualized. Twin pairs with larger differences in IQ scores tended to have more loci identified by screening for epigenetically regulated genes.
(TIF)

**Figure S3 PCA results for the expression profiles of 17 twin pairs.** Principle components ranked from the highest variance are named accordingly as PC 1st and PC 2nd. The PCA projection maps these two components data to 2 dimensions for visualization. In the scatter plots, each point represents a sample. The color of the symbol represents the relative IQ scores with red as higher and blue as lower. The number on each symbol indicates the twin pair ID. In contrast to the similarity between co-twins from each pair, no apparent gathering pattern could be recognized by the relative IQ scores.
(TIF)

**Figure S4 Clustering analysis for the expression profiles of 17 twin pairs.** Clustering analysis for the list of 644 genes manifesting more than a 1.1-fold change between the groups of twins with higher IQ scores and the groups of their co-twins under ANOVA analysis was performed. The number below each symbol indicates the twin pair ID. The color red and blue of the symbol indicate respectively the higher IQ and the lower IQ twin of each twin pair. The scale represents fold changes, according to the color map at the bottom of the figure. No apparent clustering could be recognized.
(TIF)

**Table S1 Summary of candidate loci with methylation changes identified by promoter DNA methylation patterns and their bisulfite sequencing result.**
(DOC)

**Table S2 Up-regulated gene sets in the group of twins identified by GSEA (FDR $q$-value<0.25).**
(DOC)

**Table S3 Methylation profiling by bisulfite sequencing for *IGF1* (Chr2:101335584–131398508) in Twin Pair ID 7.**
(DOC)

## Acknowledgments

We deeply thank all the study subjects. The data discussed in this publication have been deposited in NCBI's Gene Expression Omnibus and are accessible through GEO Series accession number GSE33478. This research was supported by JST, CREST.

## Author Contributions

Conceived and designed the experiments: CCY MF KK TT. Performed the experiments: CCY MF. Analyzed the data: CCY MF. Contributed reagents/materials/analysis tools: CS PCC JS HS KI TK JA. Wrote the paper: CCY MF KK TT.

## References


1. Deary I, Whalley LJ, Lemmon H, Crawford JR, Starr JM (2000) The stability of individual differences in mental ability from childhood to old age: follow-up of the 1932 scottish mental survey. Intelligence 28:49–55.
2. Deary IJ, Yang J, Davies G, Harris SE, Tenesa A, et al. (2012) Genetic contributions to stability and change in intelligence from childhood to old age. Nature 482:212–215.
3. Wright M, Geus ED, Ando J, Luciano M, Posthuma D, et al. (2001) Genetics of cognition: outline of a collaborative twin study. Twin Res 4:48–56.
4. Jacobs N, Gestel SV, Derom C, Thiery E, Vernon P, et al. (2001) Heritability estimates of intelligence in twins: effect of chorion type. Behav Genet 31:209–217.
5. Haworth CM, Wright MJ, Martin NW, Martin NG, Boomsma DI, et al. (2010) A twin study of the genetics of high cognitive ability selected from 11,000 twin pairs in six studies from four countries. Behav Genet 39:359–370.
6. Payton A (2009) The impact of genetic research on our understanding of normal cognitive ageing: 1995 to 2009. Neuropsychol Rev 19:451–477.
7. Vinkhuyzen AA, van der Sluis S, Posthuma D (2011) Life events moderate variation in cognitive ability (g) in adults. Mol Psychiatry 16:4–6.
8. Inlow JK, Restifo LL (2004) Molecular and comparative genetics of mental retardation. Genetics 166:835–881.
9. Davies G, Tenesa A, Payton A, Yang J, Harris SE, et al. (2011) Genome-wide association studies establish that human intelligence is highly heritable and polygenic. Mol Psychiatry 16: 996–1005.
10. Bruder CE, Piotrowski A, Gijsbers AA, Andersson R, Erickson S, et al. (2008) Phenotypically concordant and discordant monozygotic twins display different DNA copy-number-variation profiles. Am J Hum Genet 82:763–771.
11. Biousse V, Brown MD, Newman NJ, Allen JC, Rosenfeld J, et al. (1997) De novo 14484 mitochondrial DNA mutation in monozygotic twins discordant for Leber's hereditary optic neuropathy. Neurology 49:1136–1138.
12. Baranzini SE, Mudge J, van Velkinburgh JC, Khankhanian P, Khrebtukova I, et al. (2010) Genome, epigenome and RNA sequences of monozygotic twins discordant for multiple sclerosis. Nature 464:1351–1356.
13. Haggarty P, Hoad G, Harris SE, Starr JM, Fox HC, et al. (2010) Human intelligence and polymorphisms in the DNA methyltransferase genes involved in epigenetic marking. PLoS One 5:e11329.
14. Holliday R (2006) Epigenetics: A Historical Overview. Epigenetics 1:76–80.
15. Javierre BM, Fernandez AF, Richter J, Al-Shahrour F, Martin-Subero JI, et al. (2010) Changes in the pattern of DNA methylation associate with twin discordance in systemic lupus erythematosus. Genome Res 20:170–179.
16. Shikishima C, Ando J, Ono Y, Toda T, Yoshimura K (2006) Registry of adolescent and young adult twins in the Tokyo area. Twin Res Hum Genet 9:811–816.
17. Plomin R, Defries JC (1980) Genetics and intelligence: recent data. Intelligence 4:15–24.
18. Johnson WE, Li W, Meyer CA, Gottardo R, Caroll JS, et al. (2006) Model-based analysis of tiling-arrays for ChIP-chip. Proc Natl Acad Sci USA 103:12457–12462.
19. Subramanian A, Tamayo P, Mootha VK, Mukherjee S, Ebert BL, et al. (2005) Gene set enrichment analysis: a knowledge-based approach for interpreting genome-wide expression profiles. Proc Natl Acad Sci USA 102:15545–15550.
20. van Nleuwpoort IC, Drent Ml (2008) Cognition in the adults with childhood-onset GH deficiency. Eur J Endocrinol 159 Suppl 1:S53–57.
21. Deary IJ, Penke L, Johnson W (2010) The neuroscience of human intelligence differences. Nat Rev Neurosci 11:201–211.
22. Shikishima C, Hiraishi K, Yamagata S, Sugimoto Y, Takemura R, et al. (2009) Is *g* an entity? A Japanese twin study using syllogisms and intelligence tests. Intelligence 37:256–267.
23. Bell JT, Spector TD (2011) A twin approach to unraveling epigenetics. Trends Genet 27:116–125.
24. Fraga MF, Ballestar E, Paz MF, Ropero S, Setien F, et al. (2005) Epigenetic differences arise during the lifetime of monozygotic twins. Proc Natl Acad Sci USA 102:10604–10609.
25. Maeda M, Hasegawa H, Hyodo T, Ito S, Asano E, et al. (2011) ARHGAP18, a GTPase-activating protein for Rho A, controls cell shape, spreading, and motility. Mol Biol Cell 22:3840–3852.
26. Govek EE, Newey SE, Akerman CJ, Cross JR, Van der Veken L, et al. (2004) The X-linked mental retardation protein oligophrenin-1 is required for dendritic spine morphogenesis. Nat Neurosci 7:364–372.
27. Potkin SG, Macciardi F, Guffanti G, Fallon JH, Wang Q, et al. (2010) Identifying gene regulatory networks in schizophrenia. NeuroImage 53:839–847.
28. Nishikawa K, Li H, Kawamura R, Osaka H, Wang YL, et al. (2003) Alterations of structure and hydrolase activity of parkinsonism-associated human ubiquitin carboxyl-terminal hydrolase L1 variants. Biochem Biophys Res Commun 304:176–183.
29. Karthikeyan S, Zhou Q, Mseeh F, Grishin NV, Osterman AL, et al. (2003) Crystal structure of human riboflavin kinase reveals a beta barrel fold and a novel active site arch. Structure 11:265–273
30. O'Brien TW, O'Brien BJ, Norman RA (2005) Nuclear MRP genes and mitochondrial disease. Gene 354:147–151.
31. Tuteja N (2003) Plant DNA helicases: the long unwinding road. J Exp Bot 54:2201–2214.
32. Fisher TS, Zakian VA (2005) Ku: a multifunctional protein involved in telomere maintenance. DNA Repair (Amst) 4:1215–1226.
33. Davydov V, Hansen LA, Shackelford DA (2003) Is DNA repair compromised in Alzheimer's disease? Neurobiol Aging 24:953–968.
34. Zekri L, Chebli K, Tourrière H, Nielsen FC, Hansen TV, et al. (2005) Control of fetal growth and neonatal survival by the RasGAP-associated endoribonuclease G3BP. Mol Cell Biol 25:8703–8716.
35. Thiel CM, Fink GR (2008) Effects of the cholinergic agonist nicotine on reorienting of visual spatial attention and top-down attentional control. Neuroscience 152:381–390.
36. Nakauchi S, Brennan RJ, Boulter J, Sumikawa K (2007) Nicotine gates long-term potentiation in the hippocampal CA1 region via the activation of alpha2* nicotinic ACh receptors. Eur J Neurosci 25:2666–2681.
37. Brown BS, Yu SP (2000) Modulation and genetic identification of the M channel. Prog Biophys Mol Biol 73:135–166.
38. Peters HC, Hu H, Pongs O, Storm JF, Isbrandt D (2005) Conditional transgenic suppression of M channels in mouse brain reveals functions in neuronal excitability, resonance and behavior. Nat Neurosci 8:51–60.
39. Buxton A, Callan OA, Blatt EJ, Wong EH, Fontana DJ (1994) Cholinergic agents and delay-dependent performance in the rat. Pharmacol Biochem Behav 49:1067–1073.
40. Rodriguez S, Gaunt TR, Day INM (2007) Molecular genetics of human growth hormone, insulin-like growth factors and their pathways in common disease. Hum Genet 122:1–21.
41. Butcher LM, Meaburn E, Knight J, Sham PC, Schalkwyk LC, et al. (2005) SNPs, microarrays and pooled DNA: identification of four loci associated with mild mental impairment in a sample of 6000 children. Hum Mol Genet 14:1315–1325.
42. Bilder RM, Sabb FW, Cannon TD, London ED, Jentsch JD, et al. (2009) Phenomics: the systematic study of phenotypes on a genome-wide scale. Neuroscience 164:30–42.
43. Lister R, Pelizzola M, Dowen RH, Hawkins RD, Hon G, et al. (2009) Human DNA methylomes at base resolution show widespread epigenomic differences. Nature 462:351–322.
44. Glatt SJ, Everall IP, Kremen WS, Corbeil J, Sásik R, et al. (2005) Comparative gene expression analysis of blood and brain provides concurrent validation of *SELENBP1* up-regulation in schizophrenia. Proc Natl Acad Sci U S A 102:15533–15538.
45. Cai C, Langfelder P, Fuller TF, Oldham MC, Luo R, et al. (2010) Is human blood a good surrogate for brain tissue in transcriptional studies? BMC Genomics 11:589.
46. Sullivan PF, Fan C, Perou CM (2006) Evaluating the comparability of gene expression in blood and brain. Am J Med Genet B Neuropsychiatr Genet 141B:261–268.
47. Dempster EL, Pidsley R, Schalkwyk LC, Owens S, Georgiades A, et al. (2011) Disease-associated epigenetic changes in monozygotic twin discordant for schizophrenia and bipolar disorder. Hum Mol Genet 20:4786–4796.
48. Nguyen AT, Rauch TA, Pfeifer GP, Hu VW (2010) Global methylation profiling of lymphoblastoid cell lines reveals epigenetic contributions to autism spectrum disorders and a novel autism candidate gene, *RORA*, whose protein product is reduced in autistic brain. FASEB J 24:3036–3051.
49. Sugawara H, Iwamoto K, Bundo M, Ueda J, Miyauchi T, et al. (2011) Hypermethylation of serotonin transporter gene in bipolar disorder detected by epigenome analysis of discordant monozygotic twins. Transl Psychiatry 1:e24.
50. Schroeder DI, Lott P, Korf I, Laselle JM (2011) Large-scale methylation domains mark a functional subset of neuronally expressed genes. Genome Res 21:1583–1591.
51. Dallas PB, Gottardo NG, Firth MJ, Beesley AH, Hoffmann K, et al. (2005) Gene expression levels assessed by oligonucleotide microarray analysis and quantitative real-time RT-PCR – how well do they correlate? BMC Genomics 6:59.
52. Mathers JC, Strathdee G, Relton CL (2010) Induction of epigenetic alterations by dietary and other environmental factors. Adv Genet 71:3–39.

OPEN ACCESS

SHORT REPORT

# A multi-centre clinico-genetic analysis of the VPS35 gene in Parkinson disease indicates reduced penetrance for disease-associated variants

Manu Sharma,[1CA] John P A Ioannidis,[2] Jan O Aasly,[3] Grazia Annesi,[4] Alexis Brice,[5,6,7] Lars Bertram,[8] Maria Bozi,[9,10,11] Maria Barcikowska,[12] David Crosiers,[13,14,15] Carl E Clarke,[16] Maurizio F Facheris,[17] Matthew Farrer,[18] Gaetan Garraux,[19] Suzana Gispert,[20] Georg Auburger,[19] Carles Vilariño-Güell,[18] Georgios M Hadjigeorgiou,[21] Andrew A Hicks,[17] Nobutaka Hattori,[22] Beom S Jeon,[23] Zygmunt Jamrozik,[24] Anna Krygowska-Wajs,[25] Suzanne Lesage,[5,6,7] Christina M Lill,[9,26] Juei-Jueng Lin,[27] Timothy Lynch,[28] Peter Lichtner,[29] Anthony E Lang,[30] Cecile Libioulle,[18] Miho Murata,[31] Vincent Mok,[32] Barbara Jasinska-Myga,[33] George D Mellick,[34] Karen E Morrison,[17,35] Thomas Meitnger,[36,37] Alexander Zimprich,[38] Grzegorz Opala,[36] Peter P Pramstaller,[19] Irene Pichler,[19] Sung Sup Park,[26] Aldo Quattrone,[4] Ekaterina Rogaeva,[39] Owen A. Ross,[40] Leonidas Stefanis,[11,41] Joanne D Stockton,[35] Wataru Satake,[42] Peter A Silburn,[43] Tim M Strom,[37,39] Jessie Theuns,[14,15] Eng- King Tan,[44] Tatsushi Toda,[42] Hiroyuki Tomiyama,[22] Ryan J Uitti,[45] Christine Van Broeckhoven,[14,15] Karin Wirdefeldt,[46] Zbigniew Wszolek,[45] Georgia Xiromerisiou,[21] Harumi S Yomono,[47] Kuo-Chu Yueh,[27] Yi Zhao, Thomas Gasser,[1] Demetrius Maraganore,[48] Rejko Krüger,[1] on behalf of GEOPD consortium

► Additional supplementary files are published online only. To view these files please visit the journal online (http://dx.doi.org/10.1136/jmedgenet-2012-101155).

For numbered affiliations see end of article

**Correspondence to**
Dr Manu Sharma, Department. of Neurodegenerative diseases, Hertie-Institute for Clinical Brain Research and DZNE- German Center for Neurodegenerative Diseases, Tübingen, Hoppe-Seyler-Str. 3, Tübingen 72076, Germany; manu.sharma@uni-tuebingen.de

Additional supplementary tables are published online only. To view these files please visit the journal online (http://dx.doi.org/10.1136/jmedgenet-2012-101155).

Received 6 July 2012
Revised 5 September 2012
Accepted 7 September 2012

## ABSTRACT

**Background** Two recent studies identified a mutation (p.Asp620Asn) in the vacuolar protein sorting 35 gene as a cause for an autosomal dominant form of Parkinson disease . Although additional missense variants were described, their pathogenic role yet remains inconclusive.

**Methods and results** We performed the largest multi-center study to ascertain the frequency and pathogenicity of the reported vacuolar protein sorting 35 gene variants in more than 15,000 individuals worldwide. p.Asp620Asn was detected in 5 familial and 2 sporadic PD cases and not in healthy controls, p.Leu774Met in 6 cases and 1 control, p.Gly51Ser in 3 cases and 2 controls. Overall analyses did not reveal any significant increased risk for p.Leu774Met and p.Gly51Ser in our cohort.

**Conclusions** Our study apart from identifying the p. Asp620Asn variant in familial cases also identified it in idiopathic Parkinson disease cases, and thus provides genetic evidence for a role of p.Asp620Asn in Parkinson disease in different populations worldwide.

## INTRODUCTION

There is increasing interest to try to identify uncommon and rare genetic variants that increase the risk of common diseases and that are difficult to identify using traditional genome-wide association studies (GWAS) approaches.[1] Rare variants which are not mapped by GWAS can be identified by using next generation sequencing, that is, exome sequencing in large families with multiple affected individuals.[2] Exome sequencing is now routinely used to identify rare mutations in familial forms of disease in diverse phenotypes.[2]

Two recent studies independently performed exome sequencing in large families of Caucasian descent, and identified a mutation in the vacuolar protein sorting 35 (VPS35) gene as a possible cause for an autosomal dominant form of Parkinson disease (PD).[3 4] In addition, several non-synonymous base exchanges were identified, but their involvement in disease pathogenesis remains inconclusive. Furthermore, recently published studies provided conflicting results regarding the role of VPS35 in PD.[5–8] Here, we performed a large multi-centre study to determine the frequency and pathogenicity of VPS35 variants in PD in diverse populations worldwide.

## METHODS

### Consortium

Investigators from the Genetic Epidemiology of Parkinson disease Consortium were invited to participate in this study. A total of 23 sites representing 19 countries from four continents agreed to contribute DNA samples and clinical data for a total of 15 383 individuals (8870 cases and 6513 controls). Control individuals underwent neurological examination and were excluded from the study whenever there was clinical evidence for any extrapyramidal disorder.

### Genotyping

We selected seven non-synonymous variants exactly as they were proposed.[3] In addition, we selected tag single nucleotide polymorphisms

(SNPs) (HapMap Rel 28 phase II+III, Aug10, National Centre for Biotechnology Information. B36 dbSNP b126; http://www.hapmap.org) that cover the common genetic variants in the VPS35 gene using an $r^2$ threshold of 0.8–1.0 to select tag SNPs for VPS35 gene. Using this strategy, we were able to capture 23 SNPs in a 40 kb region, including VPS35 ('chr16:46 693 589–46 723 144 based on hg 19'). Therefore, in total, 10 SNPs located in the VPS35 were genotyped (including seven rare non-synonymous and three common variants). Genotyping was performed by a central genotyping core. Genotyping was performed using a matrix-assisted laser desorption/ionisation time-of-flight mass spectrometry on a MassArray system (Sequenom, San Diego, California, USA). Cleaned extension products were analysed by a mass spectrometer (Bruker Daltronic, Billerica, MA, USA) and peaks were identified using the MassArray Typer 4.0.2.5 software (Sequenom). Assays were designed by the AssayDesigner software 4.0 (Sequenom) with the default parameters for the iPLEX Gold chemistry and the Human GenoTyping Tools ProxSNP and PreXTEND (Sequenom). All variants were genotyped in one multiplex assay. The average call rate of the variants was >97%. The local Ethics Committee approved the study. All participants gave signed informed consent.

### Statistical analysis

Logistic regression was used to test the association between VPS35 and PD in our overall cohort. For common variants (minor allele frequency >5%), we synthesised the effect estimates using fixed and random effects models. Fixed effect models assume that the genetic effect is the same in populations from different sites and that observed differences are due to chance alone. For associations showing between-study heterogeneity, fixed effect estimates yield narrower CIs and smaller p values as compared with random effects models, which incorporate between-study heterogeneity.[9 10] Random effects models allow the genetic effects might be different due to genuine heterogeneity that may exist across different sites. Random effects calculations take into account the estimated between-study heterogeneity. Cochran's Q test of homogeneity and the $I^2$ metric were used to evaluate the between-site heterogeneity. The $I^2$ metric ranges from 0% to 100% and measures the proportion of variability that is beyond chance. Typically, estimates of $I^2$<25% are considered to reflect little or no heterogeneity, 25%–50% moderate heterogeneity, 50%–75% large heterogeneity and >75% very large heterogeneity. The overall main analysis considered all sites and populations irrespective of ancestry. For variants with minor allele frequency <1%, an exact test was used to compare the frequency differences between cases and controls combining data across all 21 sites.

## RESULTS

### Characteristics of sites and overall database

Overall, 23 sites contributed a total of 8870 cases and 6513 controls. Characteristics of all participating sites are shown in table 1. Most sites contributed participants of Caucasian ancestry (N=19); four sites included participants of Asian ancestry. The proportion of men and women ranged from 42% to 58% across different participating sites (table 1). The median age at onset of PD in our studied population was 61 years.

### Rare variants

Overall, we observed p.Asp620Asn in seven cases, p.Leu774Met in six cases and one control, p.Gly51Ser in three cases and two controls. Details per site are shown in table 2. The controls subjects carrying p.Leu774Met (P-13) and p.Gly51Ser (P-2 and P-16) at the time of study sampling were 81, 84 and 76 years, respectively. In Caucasian populations, the number of carriers in cases and controls for the three variants were 5 versus 0 (pAsp620Asn), 4 versus 1 (pLeu774Met) and 3 versus 1 (p.Gly51Ser), respectively. In Asian descent populations, the respective numbers were 2 versus 0 (p.Asp620Asn), 2 versus 0 (p.Leu774Met) and 0 versus 1 (p.Gly51Ser). Most interestingly, two out of seven patients carrying the p.Asp620Asn variant presented without any family history for PD. This represents the first evidence for reduced penetrance of the respective variant initially attributed to autosomal dominant familial PD. We did not observe any carriers for one variant (p.Arg524Trp) in our cohort. Two non-synonymous variants (p.Met57Ile, p.Thr82Arg) failed genotyping. By collapsing the rare variants across different sites, we did not observe statistically significant increased risk for p.Leu774Met and p.Gly51Ser in our cohort (see online supplementary table S1).

### Overall data synthesis for common variants

Out of three tag SNPs, one SNP (rs3218745) failed genotyping. We did not observe significant association for any of common variants with PD either with either fixed effect or random effect models (see online supplementary table S2). The OR ranged from 0.96 to 0.99 and tight 95% CIs excluded modest association effects. We observed no substantial heterogeneity for the two genotyped SNPs, and also the Q test was non-statistically significant for common SNPs. Moreover, examining the Caucasian or Asian populations separately did not change our results (data not shown).

### Clinical features

All PD patients who carried potential pathogenic variants (p.Asp620Asn, p.Gly51Ser, p.Leu774Met) were clinically diagnosed with PD (Online supplementary clinical analysis data). A few of these (0.2%) affected individuals also have a positive family history. Affected individuals exhibited classical symptoms of PD (resting tremor, bradykinesia, rigidity) (table 2). The clinical diagnosis of PD was made by movement disorder specialists who used UK brain bank criteria for PD. Non-motor symptoms were present in the majority of PD patients carrying a pathogenic variant (table 2). Interestingly, hallucinations and dementia were also observed in one asymptomatic carrier suggesting clinical heterogeneity associated with VPS35. The identified healthy carriers have not shown any sign of PD as yet (table 2).

## DISCUSSION

We performed the first multi-centre study to define the role of the VPS35 gene (PARK17) in PD by assessing the frequency of the reported non-synonymous variants in familial and sporadic PD patients from different populations worldwide. Among 15 383 subjects genotyped, we found a pathogenic relevance for p.Asp620Asn in different populations. Most interestingly, out of seven subjects who carry p.Asp620Asn, two have a negative family history. Therefore, our results provide additional evidence that VPS35 is a rare cause of familial as well as the common sporadic form of PD. In total, about 0.4% of PD cases in diverse population were due to disease-associated variant in the VPS35 gene. Our lack of supporting the role of common variants of the VPS35 gene in PD is consistent with recently published GWAS and also meta- analyses of GWAS of PD, as none of these highlighted the role of common variability in VPS35 gene as a risk factor for PD.[11–15] The p.Asp620Asn

**Table 1** Description of datasets contributed by each study site

| Site | Country | N | Case | Control | Male (%) | Female (%) | Mean AAO | Mean Age at study | Diagnostic criteria |
|---|---|---|---|---|---|---|---|---|---|
| Annesi | Italy | 394 | 197 | 197 | 204 (51.7%) | 190 (48.2%) | 61.5 | 63.7 | UKPDBB |
| Brice | France | 505 | 272 | 233 | 302 (59.8%) | 203 (40.1%) | 47.6 | 57.8 | UKPDBB |
| Bozi | Greece | 222 | 114 | 108 | 107 (48.1%) | 115 (51.8%) | 69.9 | 74.5 | UKPDBB |
| Wszolek | USA | 1518 | 692 | 826 | 794 (52.3%) | 724 (47.6%) | 64.4 | 71.7 | UKPDBB |
| Garraux | Belgium | 82 | 68 | 14 | 45 (54.8) | 37 (45.1%) | 62.1 | 69.6 | UKPDBB |
| Hadjigeorgiou | Greece | 714 | 357 | 357 | 379 (53.0%) | 335 (46.9%) | 63.4 | 63.7 | UKPDBB |
| Jeon | Korea | 749 | 408 | 341 | 314 (41.9%) | 435 (58.0%) | 57.6 | NA | UKPDBB |
| Opala | Poland | 629 | 352 | 277 | 340 (54.0%) | 288 (45.7%) | 50.2 | 68.1 | UKPDBB |
| Lynch | Ireland | 740 | 368 | 372 | 340 (45.9%) | 400 (54.0%) | 50.5 | 70.7 | UKPDBB |
| Lin | Taiwan | 320 | 160 | 160 | 160 (50%) | 160 (50%) | 62.0 | 70.8 | UKPDBB |
| Facheris | Italy | 181 | 114 | 67 | 86 (47.5%) | 95 (52.4%) | 63.0 | NA | UKPDBB |
| Maraganore | USA | 1024 | 801 | 223 | 600 (58.5%) | 361 (35.3%) | 59 | 74.7 | Bower |
| Mellick | Australia | 2024 | 1012 | 1012 | 1042 (51.4%) | 981 (48.4%) | 59 | 72.2 | Bower |
| Morrison | England | 1120 | 766 | 354 | 606 (54.1%) | 514 (45.8%) | 66.1 | NA | UKPDBB |
| Mok | China | 436 | 260 | 176 | 264 (60.5%) | 170 (38.9%) | NA | 63.5 | UKPDBB |
| Aasly | Norway | 1278 | 656 | 622 | 721 (56.4%) | 557 (43.5%) | 58.8 | 72.9 | UKPDBB |
| Wirdefeldt | Sweden | 299 | 83 | 216 | 147 (49.1%) | 152 (50.8%) | 65.8 | 71.4 | Gelb |
| Van Broeckhoven | Belgium | 1010 | 501 | 509 | 500 (49.5%) | 509 (50.3%) | 60.5 | 66.3 | Pals/Gelb |
| Rogaeva | Canada | 560 | 387 | 173 | 303 (54.1%) | 257 (45.8%) | 49.7 | 64.2 | UKPDBB |
| Tan | Singapore | 391 | 194 | 197 | 244 (62.4%) | 147 (37.5%) | 59.7 | 54.0 | UKPDBB |
| Hattori | Japan | 121 | 121 | 0 | 62 (51.2%) | 59 (48.7%) | NA | NA | UKPDBB |
| Gasser/Sharma | Germany | 760 | 760 | 0 | 479 (63.3%) | 281 (36.9%) | 58.9 | NA | UKPDBB |
| Toda | Japan | 306 | 227 | 79 | 161 (52.6%) | 145 (47.3%) | 57.8 | 65.1 | UKPDBB |
| Total | | **15 383** | **8870** | **6513** | | | 59.5 | 67.6 | |

AAO, Age at onset; NA: Not applicable.

variant is located in the C-terminal region of the VPS35 protein pointing that subtle structural changes might influence the disease pathogenesis.[3]

The spectrum of proteins involved in PD aetiology has grown considerably. This includes proteins that are related to mitochondrial quality control (Parkin, PINK1 and DJ1), proteins involved in protein aggregation (SNCA) (Synuclein, MAPT) Microtubule associated protein Tau), and proteins which are involved in sorting and degradation within endocytic and autophagy pathways ((VDAC) Voltage dependent anion channel, (GBA) Glucocerebrosidase gene, VPS35).[16 17] So far, very little is known about the specific role of VPS35 in PD, except that it is hypothesised that it is involved in cargo recognition as part of a retrograde complex recycling membrane proteins from endosomes to the trans-Golgi network.[3 4] Indeed, in vitro and in vivo studies strongly implicate the role of VPS35

**Table 2** Clinical description of carriers of non-synonymous variants of vacuolar protein sorting 35 gene

| Id | Ethnicity | Rare variant | Age at onset | Clinical signs | Bradykinesia | Rigidity | Tremor | Postural instability | L-dopa responsive | Non-motor symptoms | Family history |
|---|---|---|---|---|---|---|---|---|---|---|---|
| P-1 | Caucasian | p.Asp620Asn | 59 | Classical PD | + | + | + | + | + | Negative | Negative |
| P-2 | Caucasian | p.Gly51Ser | NA | Control | – | – | – | – | – | Negative | Negative |
| P-3 | Caucasian | p.Gly51Ser | NAV | Classical PD | + | + | + | + | + | Dementia, visual hallucinations | Negative |
| P-4 | Caucasian | p.Gly51Ser | 55 | Classical PD | + | + | + | + | + | Negative | Negative |
| P-5 | Caucasian | p.Gly51Ser | 49 | Classical PD | + | + | + | + | + | Negative | Negative |
| P-6 | Caucasian | p.Asp620Asn | 37 | Classical PD | + | + | + | + | + | Negative | Positive |
| P-7 | Caucasian | p.Asp620Asn | 59 | Classical PD | + | + | + | + | + | Negative | Positive |
| P-8 | Caucasian | p.Asp620Asn | 55 | Classical PD | + | + | + | + | + | Negative | Positive |
| P-9 | Caucasian | p.Asp620Asn | 66 | Classical PD | + | + | + | + | + | Negative | Positive |
| P-10 | Caucasian | p.Leu774Met | 41 | Classical PD | + | + | + | + | + | Negative | Positive |
| P-11 | Caucasian | p.Leu774Met | 65 | Classical PD | + | + | + | + | + | Negative | Positive |
| P-12 | Caucasian | p.Leu774Met | 65 | Classical PD | + | + | + | + | + | Disturbance of gait and balance | Positive |
| P-13 | Caucasian | p.Leu774Met | NA | Control | – | – | – | – | NA | - | Negative |
| P-14 | Caucasian | p.Leu774Met | 44 | Classical PD | + | + | + Rest 1st sx | + | + | Autonomic dysfunction | Positive |
| P-15 | Asian | p.Asp620Asn,p. Leu774Met | 52 | Classical PD | + | + | + | + | + | Negative | Negative |
| P-16 | Asian | p.Gly51Ser | | Control | – | – | – | – | – | – | Negative |
| P-17 | Asian | p.Leu774Met | 75 | Classical PD | + | + | + | + | + | Negative | Negative |
| P-18 | Asian | p.Asp620Asn | 43 | Classical PD | + | + | + | + | + | Mild cognitive impairment | Positive |

NA, not applicable; NAV, not available; PD, Parkinson disease; +positive; –negative.

gene in neurodegeneration. For example, reduced levels of VPS35 have been found in affected brain regions of Alzheimer disease (AD) patients[18] and loss of VPS35 function has been shown to increase the levels of amyloid β and cause synaptic impairment in a mouse model of AD. Furthermore, variants in another member of the VPS family and substrate of retromer complex, SORL1, have been implicated in AD.[19]

In this study, we have focused only on non-synonymous variants identified by Zimprich and colleagues.[3] Of note, we confirmed the pathogenic relevance of the p.Asp620Asn variant which was identified by both studies for familial cases and in sporadic PD. Recently, published studies also identified p.Asp620Asn mutations in PD,[6 20] thus providing support to the role of p.Asp620Asn in PD. In our study, clinically, the symptomatic carriers showed a broad spectrum of clinical phenotypes ranging from typical PD to (DLB) Dementia with Lewy body, so longitudinal evaluation of carriers at risk will provide unique information on the natural course of the disease caused by VPS35. Even though our data support the role of p.Asp620Asn variant in PD, given the fact that the frequency in diverse population is far below <1%, it is likely to be a rare cause of PD worldwide. Nevertheless, sequencing of families is encouraged for identifying additional missense variants which may provide mechanistic insight into the causes of PD.

**Author affiliations**
[1]Department of Neurodegenerative diseases, Hertie-Institute for Clinical Brain Research and DZNE- German Center for Neurodegenerative Diseases, Tübingen
[2]Stanford Prevention Research Center, Department of Medicine and Department of Health Research and Policy, Stanford University School of Medicine, Stanford, California, USA
[3]Department of Neurology, St Olavs Hospital and NTNU Trondheim, Trondheim, Norway
[4]Institute of Neurology, Department of Medical Sciences , University Magna Graecia, Catanzaro; Neuroimaging Research Unit, National Research Council, Catanzaro, Italy
[5]INSERM, UMR_S975, Université Pierre et Marie Curie-Paris, CNRS, UMR 7225, AP-HP, Pitié-Salpêtrière Hospital
[6]Cnrs, UMR 7225, Paris, France
[7]AP-HP, Hôpital Pitié-Salpêtière, Department of Genetics and Cytogenetics, Paris, France
[8]Neuropsychiatric Genetics Group, Department of Vertebrate Genomics, Max Planck Institute for Molecular Genetics, Berlin, Germany.
[9]General Hospital of Syros, Syros, Greece
[10]'Hygeia' Hospital, Clinic of Neurodegenerative Disorders, Athens, Greece
[11]2nd Neurology Clinic, University of Athens, 'Attikon' Hospital, Athens, Greece
[12]Department of Neurodegenerative Disorders, Medical Research Centre, Polish Academy of Sciences, Warsaw, Poland
[13]Neurodegenerative Brain Diseases Group, Department of Molecular Genetics, VIB, Antwerp, Belgium
[14]Institute Born-Bunge, University of Antwerp, Antwerp, Belgium
[15]Department of Neurology, Antwerp University Hospital, Antwerp, Belgium.
[16]School of Clinical and Experimental Medicine, College of Medical and Dental Sciences, University of Birmingham, City Hospital, Birmingham, UK
[17]Centre for Biomedicine, European Academy Bozen/Bolzano, Itlay, Affiliated institute of the University of Lübeck, Lübeck, German
[18]Department of Medical Genetics, University of British Columbia, Vancouver, British Columbia, Canada
[19]Human Genetic Centre, University Hospital of Liège, Liège, Belgium and Department of Neurology, General Central Hospital, Bolzano, Itlay
[20]Department of Neurology, Goethe University Frankfurt am Main, Frankfurt, Germany
[21]Department of Neurology, University of Thessaly and Institute of Biomedical Research and Technology, CERETETH, Larissa, Greece
[22]Department of Neurology, Juntendo University School of Medicine, Tokyo, Japan
[23]Department of Neurology, Seoul National University Hospital, Seoul, Korea
[24]Department of Neurology, Medical University of Warsaw, Warsaw, Poland
[25]Department of Neurology, Jagiellonian University, Krakow, Poland
[26]Department of Neurology, Johannes Gutenberg University, Mainz, Germany
[27]Department of Neurology, Chushang Show-Chwan Hospital, Nantou and Chung-Shan Medical University Hospital, Taichung, Taiwan
[28]The Dublin Neurological Institute at the Mater Misericordiae University Hospital, and Conway Institute, University College Dublin, Dublin, Ireland
[29]Helmholtz Zentrum München, German Research Centre for Environmental Health (Gmbh), Neuherberg, Germany
[30]Movement Disorders Centre, and the Edmond J Safra Program in Parkinson's Disease, Toronto Western Hospital, University of Toronto, Toronto, Canada
[31]Department of Neurology, National Center Hospital of Neurology and Psychiatry, Tokyo, Japan
[32]Department of Medicine and Therapeutics, Prince of Wales Hospital,The Chinese University of Hong Kong, Shatin, Hong Kong
[33]Department of Neurology, Medical University of Silesia, Katowice, Poland
[34]Eskitis Institute for Cell and Molecular Therapies, Griffith University, Brisbane, Australia
[35]Neurosciences Department, Queen Elizabeth Hospital Birmingham, University Hospitals Birmingham NHS Foundation Trust, Birmingham, UK
[36]German Research Center for Environmental Health, Institute of Human Genetics, Helmholtz Zentrum München, Neuherberg, Germany
[37]Institute of Human Genetics, Technische Universität München, Munich, Germany
[38]Department of Neurology, Medizinische Universität Wien, Vienna, Austria
[39]Tanz Centre for Research in Neurodegenerative Diseases, Department of Medicine, University of Toronto, Toronto, Canada
[40]Department of Neuroscience, Mayo Clinic, Jacksonville, Florida
[41]Divisions of Basic Neurosciences & Cell Biology, Biomedical Research Foundation of Academy of Athens, Athens, Greece
[42]Division of Neurology/Molecular Brain Science, Kobe University Graduate School of Medicine, Kobe, Japan
[43]University of Queensland Centre for Clinical Research, Herston, Australia
[44]Department of Neurology, Singapore General Hospital, National Neuroscience Institute, Singapore
[45]Department of Neurology, Mayo Clinic Jacksonville, USA
[46]Epidemiology and Biostatistics and Department of Clinical Neuroscience, Karolinska Institutet
[47]Department of Neurology, National Hospital Organization Tokyo Hospital, Tokyo, Japan
[48]Department of Neurology, NorthShore University HealthSystem, Chicago, USA

**Acknowledgements** RS Boyle, MD (Princess Alexandra Hospital, Brisbane, Site Investigator); A Sellbach, MD (Princess Alexandra Hospital, Brisbane, Site Investigator); JD O'Sullivan, MD (Royal Brisbane and Women's Hospital Brisbane, Site Investigator); GT Sutherland, PhD (Eskitis Institute for Cell and Molecular Therapies, Griffith University, Nathan, QLD, Site Investigator); GA Siebert, MD (Eskitis Institute for Cell and Molecular Therapies, Griffith University, Nathan, QLD, Site Investigator); NNW Dissanayaka, MD (Eskitis Institute for Cell and Molecular Therapies, Griffith University, Nathan, QLD,Site Investigator); Christine Van Broeckhoven, PhD DSc (Neurodegenerative Brain Diseases Group, Department of Molecular Genetics, VIB; and Laboratory of Neurogenetics, Institute Born-Bunge; and University of Antwerp); Jessie Theuns, PhD (Neurodegenerative Brain Diseases Group, Department of Molecular Genetics, VIB; and Laboratory of Neurogenetics, Institute Born-Bunge; and University of Antwerp); David Crosiers, MD (Neurodegenerative Brain Diseases Group, Department of Molecular Genetics, VIB; and Laboratory of Neurobiology, Institute Born-Bunge; and University of Antwerp; and Department of Neurology, Antwerp University Hospital, Antwerp); Barbara Pickut, MD (Department of Neurology, Antwerp University Hospital, Antwerp); Sebastiaan Engelborghs, MD, PhD (Laboratory of Neurochemistry and Behaviour, Institute Born-Bunge; and University of Antwerp; and Department of Neurology and Memory Clinic, Hospital Network Antwerp, Middelheim and Hoge Beuken, Antwerp); Aline Verstraeten (Neurodegenerative Brain Diseases Group, Department of Molecular Genetics, VIB; and Laboratory of Neurogenetics, Institute Born-Bunge; and University of Antwerp); Peter P De Deyn, MD, PhD (Laboratory of Neurochemistry and Behaviour, Institute Born-Bunge; and University of Antwerp; and Department of Neurology and Memory Clinic, Hospital Network Antwerp, Middelheim and Hoge Beuken, Antwerp; and Department of Neurology and Alzheimer Research Center, University Medical Center Groningen, The Netherlands); Patrick Cras, MD, PhD (Laboratory of Neurobiology, Institute Born-Bunge; and University of Antwerp; Department of Neurology, Antwerp University Hospital, Antwerp). Funding: The research was in part supported by the Methusalem excellence program of the Flemish Government; a Centre of Excellence grant by the Special Research Fund of the University of Antwerp; the Research Foundation Flanders (FWO); the Agency for Innovation by Science and Technology Flanders (IWT); the Interuniversity Attraction Poles program (IAP) P6/43 of the Belgian Science Policy Office; the Belgian Parkinson Foundation; and the Foundation for Alzheimer Research (SAO/FRMA). DC is receiving a PhD fellowship of the FWO and AV of the IWT. Ekaterina Rogaeva, PhD (Tanz Centre for Research in Neurodegenerative Diseases, Department of Medicine, Division of Neurology, University of Toronto, ON, Canada, Site Investigator); Anthony E Lang, MD (Movement Disorders Centre, Toronto Western Hospital, University of Toronto, Toronto, ON, Canada, Site Investigator); Y Agid, MD (Inserm, Paris, From the French Parkinson's Disease Genetics Study Group, Site Investigator); M Anheim, MD (Inserm, Paris, From the French Parkinson's Disease Genetics Study Group, Site Investigator); A-M Bonnet, MD (Inserm, Paris, From the French Parkinson's Disease Genetics Study Group, Site Investigator); M Borg, MD (From the French Parkinson's Disease Genetics Study Group, Site Investigator); A Brice, MD (Paris, From the French Parkinson's Disease Genetics Study Group, Site Investigator); E Broussolle MD (From the French Parkinson's Disease Genetics Study Group, Site Investigator); JC Corvol MD (Inserm, Paris, From the

French Parkinson's Disease Genetics Study Group, Site Investigator); P Damier, MD (From the French Parkinson's Disease Genetics Study Group, Site Investigator); A Destée, MD (From the French Parkinson's Disease Genetics Study Group, Site Investigator); A Dürr, MD (Inserm U708, Paris, From the French Parkinson's Disease Genetics Study Group, Site Investigator); F Durif, MD (From the French Parkinson's Disease Genetics Study Group, Site Investigator); S Lesage, PhD (Inserm, Paris, From the French Parkinson's Disease Genetics Study Group, Site Investigator); E Lohmann, MD (Inserm, Paris, From the French Parkinson's Disease Genetics Study Group, Site Investigator); P Pollak, MD (From the French Parkinson's Disease Genetics Study Group, Site Investigator); O Rascol, MD (From the French Parkinson's Disease Genetics Study Group, Site Investigator); F Tison, MD (From the French Parkinson's Disease Genetics Study Group, Site Investigator); C Tranchant, MD (From the French Parkinson's Disease Genetics Study Group, Site Investigator); F Viallet, MD (From the French Parkinson's Disease Genetics Study Group, Site Investigator); M Vidailhet, MD (Inserm, Paris, From the French Parkinson's Disease Genetics Study Group, Site Investigator); Christophe Tzourio, MD (Inserm U708, Paris, From the French Parkinson's Disease Genetics Study Group, Site Investigator); Philippe Amouyel, MD (Inserm U744, Lille, Site Investigator); Marie-Anne Loriot, MD (Inserm UMRS775, Paris, Site Investigator); Eugénie Mutez, MD (Inserm UMR837, Service de Neurologie et de Pathologie du Mouvement CHRU de Lille, Univ Lille Nord de France, Site Investigator); Aurélie Duflot, MD (UMR837 Inserm-Univ Lille 2, CHRU de Lille, Site Investigator); Jean-Philippe Legendre, MD (Service de Neurologie et Pathologie du Mouvement, Clinique de Neurologie du CHU de Lille, Site Investigator); Nawal Waucquier, MD (Service de Neurologie et Pathologie du Mouvement, Clinique de Neurologie du CHU de Lille, Site Investigator); Thomas Gasser MD (Department of Neurology, University Hospital Tuebingen, Site Investigator); Olaf Riess MD (Department of Neurology, University Hospital Tuebingen, Site Investigator); Christine Klein, MD (Section of Clinical and Molecular Neurogenetics at the Department of Neurology, University of Lübeck, Site Investigator); Ana Djarmati, PhD (Department of Neurology, University of Lübeck, Site Investigator); Johann Hagenah, MD (Department of Neurology, University of Lübeck, Site Investigator); Katja Lohmann, PhD (Section of Clinical and Molecular Neurogenetics at the Department of Neurology, University of Lübeck, Site Investigator); Georg Auburger, MD (Department of Neurology, Goethe University Frankfurt am Main, Germany, Site Investigator); Rüdiger Hilker, MD (Department of Neurology, Goethe University Frankfurt am Main, Germany, Site Investigator); Simone van de Loo, MD (Department of Neurology, Goethe University Frankfurt am Main, Germany, Site Investigator); Efthimios Dardiotis, MD (Department of Neurology, Faculty of Medicine, University of Thessaly and Institute of Biomedical Research & Technology, CERETETH, Larissa; Site Investigator); Vaia Tsimourtou, MD (Department of Neurology, Faculty of Medicine, University of Thessaly, Larissa, Site Investigator); Styliani Ralli, MD (Department of Neurology, Faculty of Medicine, University of Thessaly, Larissa, Site Investigator); Persa Kountra, MD (Department of Neurology, Faculty of Medicine, University of Thessaly, Larissa, Site Investigator); Gianna Patramani, MD (Department of Neurology, Faculty of Medicine, University of Thessaly, Larissa, Site Investigator); Cristina Vogiatzi, MD (Department of Neurology, Faculty of Medicine, University of Thessaly, Larissa, Site Investigator); Nobutaka Hattori, MD, PhD (Department of Neurology, Juntendo University School of Medicine, Tokyo, Site Investigator); Hiroyuki Tomiyama, MD, PhD (Department of Neurology, Juntendo University School of Medicine, Tokyo, Site Investigator); Manabu Funayama, PhD (Department of Neurology, and Research Institute for Diseases of Old Age, Graduate School of Medicine, Juntendo University, Tokyo, Site Investigator); Hiroyo Yoshino, PhD (Research Institute for Diseases of Old Age, Graduate School of Medicine, Juntendo University, Tokyo, Site Investigator); Yuanzhe Li MD,PhD Research Institute for Diseases of Old Age, Graduate School of Medicine, Juntendo University, Tokyo, Site Investigator); Yoko Imamichi (Department of Neurology, Juntendo University School of Medicine, Tokyo, Site Investigator); Tatsushi Toda, MD (Division of Neurology/Molecular Brain Science, Kobe University Graduate School of Medicine, Kobe, Japan, Site Investigator); Wataru Satake, MD, PhD (Division of Neurology/ Molecular Brain Science, Kobe University Graduate School of Medicine, Kobe, Japan, Site Investigator); Tim Lynch, MD (The Dublin Neurological Institute at the Mater Misericordiae University Hospital, Clinical Investigator at the Conway Institute, University College Dublin, Ireland, Site Investigator); J Mark Gibson, MD (Department of Neurology, Royal Victoria Hospital, Belfast, Ireland, Site Investigator); Enza Maria Valente, MD, PhD (IRCCS, Casa Sollievo della Sofferenza Hospital, Mendel Institute, San Giovanni Rotondo, Site Investigator); Alessandro Ferraris, MD (IRCCS, Casa Sollievo della Sofferenza Hospital, Mendel Institute, San Giovanni Rotondo, Site Investigator); Bruno Dallapiccola, MD (Mendel Institute, Casa Sollievo della Sofferenza Hospital, Rome, Site Investigator); Tamara Ialongo, MD, PhD (Institute of Neurology, Catholic University, Rome, Site Investigator); Laura Brighina, MD, PhD (Department of Neurology, Ospedale San Gerarado, Monza, Italy, Site Investigator); Barbara Corradi, PhD (Department of Paediatrics, University of Milano-Bicocca, Monza, Site Investigator); Roberto Piolti, MD (Department of Neurology, Ospedale San Gerardo, Monza, Italy, Site Investigator); Patrizia Tarantino, PhD (Institute of Neurological Sciences, National Research Council, Site Investigator); Ferdinanda Annesi, PhD (Institute of Neurological Sciences, National Research Council, Site Investigator); Beom S Jeon, MD, PhD (Department of Neurology, Seoul National University Hospital, Site Investigator); Sung-Sup Park, MD, PhD (Department of Laboratory Medicine, Seoul National University Hospital, Site Investigator); J Aasly, MD (Department of Neurology, University of Trondheim, Norway, Site Investigator); Grzegorz Opala, MD, PhD (Department of Neurology, Aging, Degenerative and Cerebrovascular Disorders, Medical University of Silesia, Katowice; Site Investigator); Barbara Jasinska-Myga, MD, PhD (Department of Neurology, Aging, Degenerative and Cerebrovascular Disorders, Medical University of Silesia, Katowice, Site Investigator); Gabriela Klodowska-Duda, MD, PhD (Department of Neurology, Aging, Degenerative and Cerebrovascular Disorders, Medical University of Silesia, Katowice, Site Investigator); Magdalena Boczarska-Jedynak, MD, PhD (Department of Neurology, Aging, Degenerative and Cerebrovascular Disorders, Medical University of Silesia, Katowice, Site Investigator); Eng King Tan, MD, PhD (National Medical and Biomedical Research Councils, and the Duke-NUS Graduate Medical School, Singapore Millenium Foundation, Site Investigator); Andrea Carmine Belin, PhD (Department of Neuroscience, Karolinska Institutet, Stockholm, Site Investigator); Lars Olson, MD (Department of Neuroscience, Karolinska Institutet, Stockholm, Site Investigator); Dagmar Galter, PhD (Department of Neuroscience, Karolinska Institutet, Stockholm; Site Investigator); Marie Westerlund, PhD (Department of Neuroscience, Karolinska Institutet, Stockholm, Site Investigator); Olof Sydow, PhD (Department of Clinical Neuroscience, Karolinska University Hospital, Stockholm; Site Investigator); Christer Nilsson, MD, PhD (Department of Geriatric Psychiatry, Lund University; Site Investigator); Andreas Puschmann, MD (Department of Neurology, Lund University Hospital, Department of Geriatric Psychiatry, Lund University, Site Investigator); JJ Lin, MD (Department of Neurology, Cushang Show-Chwan Hospital, Taiwan, Site Investigator); Demetrius M Maraganore, MD (Department of Neurology, NorthShore Health Systems, Chicago, IL, Site Investigator); J Eric Ahlskog PhD, MD (Department of Neurology, Mayo Clinic, Rochester, MN, USA, Site Investigator); Mariza de Andrade, PhD (Department of Health Sciences Research, Mayo Clinic, Rochester, MN, USA, Site Investigator); Timothy G Lesnick, MS (Department of Health Sciences Research, Mayo Clinic, Rochester, MN, USA, Site Investigator); Walter A Rocca, MD, MPH (Departments of Neurology and Health Sciences Research, Mayo Clinic, Rochester, MN, USA, Site Investigator); Harvey Checkoway, PhD (Department of Environmental and Occupational Health Sciences, University of Washington, Seattle, WA, Site Investigator); Owen A Ross PhD (Division of Neuroscience, Mayo Clinic, Jacksonville, USA, Site Investigator); Zbigniew K Wszolek, MD (Department of Neurology, Mayo Clinic, Jacksonville, FL, Site Investigator); Ryan J Uitti, MD (Department of Neurology, Mayo Clinic, Jacksonville, FL, Site Investigator).

**Contributors** All authors presented in this study made substantial contributions to: (1) conception and design, acquisition of data, or analysis and interpretation of data; (2) drafting the article or revising it critically for important intellectual content; and (3) final approval of the version to be published.

**Funding** This work was supported by Michael J Fox Foundation under the Edmond J Safra Rapid Response Innovation Award program.

**Competing interests** None.

**Provenance and peer review** None.

## REFERENCES

1. **Ioannidis JP,** Thomas G, Daly MJ. Validating, augmenting and refining genome-wide association signals. *Nat Rev Genet* 2009;**10**:318–29.
2. **Singleton AB.** Exome sequencing: a transformative technology. *Lancet Neurol* 2011;**10**:942–6.
3. **Zimprich A,** Benet-Pages A, Struhal W, Graf E, Eck SH, Offman MN, Haubenberger D, Spielberger S, Schulte EC, Lichtner P, Rossle SC, Klopp N, Wolf E, Seppi K, Pirker W, Presslauer S, Mollenhauer B, Katzenschlager R, Foki T, Hotzy C, Reinthaler E, Harutyunyan A, Kralovics R, Peters A, Zimprich F, Brücke T, Poewe W, Auff E, Trenkwalder C, Rost B, Ransmayr G, Winkelmann J, Meitinger T, Strom TM. A mutation in VPS35, encoding a subunit of the retromer complex, causes late-onset Parkinson disease. *Am J Hum Genet* 2011;**89**:168–75.
4. **Vilarino-Guell C,** Wider C, Ross OA, Dachsel JC, Kachergus JM, Lincoln SJ, Soto-Ortolaza AI, Cobb SA, Wilhoite GJ, Bacon JA, Behrouz B, Melrose HL, Hentati E, Puschmann A, Evans DM, Conibear E, Wasserman WW, Aasly JO, Burkhard PR, Djaldetti R, Ghika J, Hentati F, Krygowska-Wajs A, Lynch T, Melamed E, Rajput A, Rajput AH, Solida A, Wu RM, Uitti RJ, Wszolek ZK, Vingerhoets F, Farrer MJ. VPS35 mutations in Parkinson disease. *Am J Hum Genet* 2011;**89**:162–7.
5. **Verstraeten A,** Wauters E, Crosiers D, Meeus B, Corsmit E, Elinck E, Mattheijssens M, Peeters K, Cras P, Pickut B, Vandenberghe R, Engelborghs S, De Deyn PP, Van Broeckhoven C, Theuns J. Contribution of VPS35 genetic variability to LBD in the Flanders-Belgian population. *Neurobiol Aging* 2012;**33**:1844 e11–3.
6. **Lesage S,** Condroyer C, Klebe S, Honoré A, Tison F, Brefel-Courbon C, Dürr A, Brice A, French Parkinson's Disease Genetics Study Group. Identification of VPS35 mutations replicated in French families with Parkinson disease. *Neurology* 2012;**78**:1449–50.
7. **Guo JF,** Sun QY, Lv ZY, Yu RL, Li K, Zhang YH, Tian JY, Xia K, Yan XX, Tang BS. VPS35 gene variants are not associated with Parkinson's disease in the mainland Chinese population. *Parkinsonism Relat Disord* 2012;**18**:983–5.
8. **Guella I,** Solda G, Cilia R, Pezzoli G, Asselta R, Duga S, Goldwurm S. The Asp620asn mutation in VPS35 is not a common cause of familial Parkinson's disease. *Mov Disord* 2012;**27**:800–1.

9. **Ioannidis JP,** Patsopoulos NA, Evangelou E. Uncertainty in heterogeneity estimates in meta-analyses. *BMJ* 2007;**335**:914–16.
10. **Higgins JP,** Thompson SG, Deeks JJ, Altman DG. Measuring inconsistency in meta-analyses. *BMJ* 2003;**327**:557–60.
11. **Nalls MA,** Plagnol V, Hernandez DG, Sharma M, Sheerin UM, Saad M, Simón-Sánchez J, Schulte C, Lesage S, Sveinbjörnsdóttir S, Stefánsson K, Martinez M, Hardy J, Heutink P, Brice A, Gasser T, Singleton AB, Wood NW. Imputation of sequence variants for identification of genetic risks for Parkinson's disease: a meta-analysis of genome-wide association studies. *Lancet* 2011;**377**:641–9.
12. **Simón-Sánchez J,** Schulte C, Bras JM, Sharma M, Gibbs JR, Berg D, Paisan-Ruiz C, Lichtner P, Scholz SW, Hernandez DG, Krüger R, Federoff M, Klein C, Goate A, Perlmutter J, Bonin M, Nalls MA, Illig T, Gieger C, Houlden H, Steffens M, Okun MS, Racette BA, Cookson MR, Foote KD, Fernandez HH, Traynor BJ, Schreiber S, Arepalli S, Zonozi R, Gwinn K, van der Brug M, Lopez G, Chanock SJ, Schatzkin A, Park Y, Hollenbeck A, Gao J, Huang X, Wood NW, Lorenz D, Deuschl G, Chen H, Riess O, Hardy JA, Singleton AB, Gasser T. Genome-wide association study reveals genetic risk underlying Parkinson's disease. *Nature genetics* 2009;**41**:1308–12.
13. **Satake W,** Nakabayashi Y, Mizuta I, Hirota Y, Ito C, Kubo M, Kawaguchi T, Tsunoda T, Watanabe M, Takeda A, Tomiyama H, Nakashima K, Hasegawa K, Obata F, Yoshikawa T, Kawakami H, Sakoda S, Yamamoto M, Hattori N, Murata M, Nakamura Y, Toda T. Genome-wide association study identifies common variants at four loci as genetic risk factors for Parkinson's disease. *Nat Genet* 2009;**41**:1303–7.
14. **Saad M,** Lesage S, Saint-Pierre A, Corvol JC, Zelenika D, Lambert JC, Vidailhet M, Mellick GD, Lohmann E, Durif F, Pollak P, Damier P, Tison F, Silburn PA, Tzourio C, Forlani S, Loriot MA, Giroud M, Helmer C, Portet F, Amouyel P, Lathrop M, Elbaz A, Durr A, Martinez M, Brice A. Genome-wide association study confirms BST1 and suggests a locus on 12q24 as the risk loci for Parkinson's disease in the European population. *Hum Mol Genet* 2011;**20**:615–27.
15. **Pankratz N,** W. Beecham GW, DeStefano AL, Dawson TM, Doheny KF, Factor SA, Hamza TH, Hung AY, Hyman BT, Ivinson AJ, Krainc D, Latourelle JC, Clark LN, Marder K, Martin ER, Mayeux R, Ross OA, Scherzer CR, Simon DK, Tanner C, Vance JM, Wszolek ZK, Zabetian CP, Myers RH, Payami H, Scott WK, Foroud T. Meta-analysis of Parkinson disease: identification of a novel locus, RIT2. *Ann Neurol* 2012;**71**:370–84.
16. **Geisler S,** Holmstrom KM, Skujat D, Fiesel FC, Rothfuss OC, Kahle PJ, Springer W. PINK1/Parkin-mediated mitophagy is dependent on VDAC1 and p62/SQSTM1. *Nat Cell Biol* 2010;**12**:119–31.
17. **Burbulla LF,** Krebiehl G, Kruger R. Balance is the challenge–the impact of mitochondrial dynamics in Parkinson's disease. *Eur J Clin Invest* 2010;**40**:1048–60.
18. **Small SA,** Kent K, Pierce A, Leung C, Kang MS, Okada H, Honig L, Vonsattel JP, Kim TW. Model-guided microarray implicates the retromer complex in Alzheimer's disease. *Ann Neurol* 2005;**58**:909–19.
19. **Rogaeva E,** Meng Y, Lee JH, Gu Y, Kawarai T, Zou F, Katayama T, Baldwin CT, Cheng R, Hasegawa H, Chen F, Shibata N, Lunetta KL, Pardossi-Piquard R, Bohm C, Wakutani Y, Cupples LA, Cuenco KT, Green RC, Pinessi L, Rainero I, Sorbi S, Bruni A, Duara R, Friedland RP, Inzelberg R, Hampe W, Bujo H, Song YQ, Andersen OM, Willnow TE, Graff-Radford N, Petersen RC, Dickson D, Der SD, Fraser PE, Schmitt-Ulms G, Younkin S, Mayeux R, Farrer LA, St George-Hyslop P. The neuronal sortilin-related receptor SORL1 is genetically associated with Alzheimer disease. *Nat Genet* 2007;**39**:168–77.
20. **Sheerin UM,** Charlesworth G, Bras J, Guerreiro R, Bhatia K, Foltynie T, Limousin P, Silveira-Moriyama L, Lees A, Wood N. Screening for VPS35 mutations in Parkinson's disease. *Neurobiol Aging* 2012;**33**:838.e1–5.

OPEN ACCESS Freely available online

PLOS ONE

# Hsp40 Gene Therapy Exerts Therapeutic Effects on Polyglutamine Disease Mice via a Non-Cell Autonomous Mechanism

**H. Akiko Popiel[1], Toshihide Takeuchi[1], Hiromi Fujita[1], Kazuhiro Yamamoto[2], Chiyomi Ito[3], Hiroshi Yamane[1], Shin-ichi Muramatsu[4], Tatsushi Toda[3], Keiji Wada[1], Yoshitaka Nagai[1,5]***

**1** Department of Degenerative Neurological Diseases, National Institute of Neuroscience, National Center of Neurology and Psychiatry, Kodaira, Tokyo, Japan, **2** Division of Laboratory Animals Resources, National Institute of Neuroscience, National Center of Neurology and Psychiatry, Kodaira, Tokyo, Japan, **3** Division of Neurology/Molecular Brain Science, Kobe University Graduate School of Medicine, Kobe, Hyogo, Japan, **4** Division of Neurology, Department of Medicine, Jichi Medical University, Shimotsuke, Tochigi, Japan, **5** Core Research for Evolutional Science and Technology (CREST), Japan Science and Technology Agency, Kawaguchi, Saitama, Japan

## Abstract

The polyglutamine (polyQ) diseases such as Huntington's disease (HD), are neurodegenerative diseases caused by proteins with an expanded polyQ stretch, which misfold and aggregate, and eventually accumulate as inclusion bodies within neurons. Molecules that inhibit polyQ protein misfolding/aggregation, such as Polyglutamine Binding Peptide 1 (QBP1) and molecular chaperones, have been shown to exert therapeutic effects *in vivo* by crossing of transgenic animals. Towards developing a therapy using these aggregation inhibitors, we here investigated the effect of viral vector-mediated gene therapy using QBP1 and molecular chaperones on polyQ disease model mice. We found that injection of adeno-associated virus type 5 (AAV5) expressing QBP1 or Hsp40 into the striatum both dramatically suppresses inclusion body formation in the HD mouse R6/2. AAV5-Hsp40 injection also ameliorated the motor impairment and extended the lifespan of R6/2 mice. Unexpectedly, we found even in virus non-infected cells that AAV5-Hsp40 appreciably suppresses inclusion body formation, suggesting a non-cell autonomous therapeutic effect. We further show that Hsp40 inhibits secretion of the polyQ protein from cultured cells, implying that it inhibits the recently suggested cell-cell transmission of the polyQ protein. Our results demonstrate for the first time the therapeutic effect of Hsp40 gene therapy on the neurological phenotypes of polyQ disease mice.

**Citation:** Popiel HA, Takeuchi T, Fujita H, Yamamoto K, Ito C, et al. (2012) Hsp40 Gene Therapy Exerts Therapeutic Effects on Polyglutamine Disease Mice via a Non-Cell Autonomous Mechanism. PLoS ONE 7(11): e51069. doi:10.1371/journal.pone.0051069

**Editor:** Hitoshi Okazawa, Tokyo Medical and Dental University, Japan

**Received** July 18, 2012; **Accepted** October 29, 2012; **Published** November 30, 2012



**Funding:** This work was supported in part by Grants-in-Aid for Scientific Research on Priority Areas (Research on Pathomechanisms of Brain Disorders and Protein Community to Y.N.), and on Innovative Areas (Synapse and Neurocircuit Pathology to Y.N. and S.M.) and by a Comprehensive Brain Science Network Award for Young Scientists to H.A.P., from the Ministry of Education, Culture, Sports, Science, and Technology, Japan; by Grants-in-Aid for Scientific Research (B) to Y.N., for Young Scientists (B) to H.A.P., from the Japan Society for the Promotion of Science, Japan; by a Grant-in-Aid for the Research Committee for Ataxic Diseases to Y.N. and a Grant-in-Aid for the Research Committee of CNS Degenerative Diseases to S.M. from the Ministry of Health, Labor and Welfare, Japan. The funders had no role in study design, data collection and analysis, decision to publish, or preparation of the manuscript.

**Competing Interests:** Co-author Yoshitaka Nagai is a PLOS ONE Editorial Board member. This does not alter the authors' adherence to all the PLOS ONE policies on sharing data and materials.

* E-mail: nagai@ncnp.go.jp

## Introduction

The polyglutamine (polyQ) diseases are a group of inherited neurodegenerative disorders that are all caused by a common genetic mutation, namely an expansion (>40) of a polyQ-encoding CAG repeat in each unrelated disease-causing gene [1,2]. Nine polyQ diseases have been identified to date, including Huntington's disease (HD), spinocerebellar ataxia (SCA) types 1, 2, 3, 6, 7, 17, dentatorubral pallidoluysian atrophy (DRPLA), and spinobulbar muscular atrophy (SBMA). In these disorders, progressive degeneration of neurons in brain areas specific for each disorder occurs, causing various neurological and psychiatric symptoms corresponding to each affected brain area [1,2].

In the common molecular pathogenesis of the polyQ diseases, proteins with an expanded polyQ stretch become misfolded and form aggregates, and subsequently accumulate as inclusion bodies within neurons, eventually resulting in neurodegeneration [3–7]. Moreover, recent studies suggest that prion-like transmission of aggregation-prone proteins between cells is involved in neuropathological spreading during disease progression in not only the polyQ diseases but also various other neurodegenerative diseases [8–11]. Although various therapeutic strategies against downstream targets of the pathogenic cascade have been investigated, misfolding and aggregation of the polyQ protein are ideal therapeutic targets since they are the most initial pathogenic events, and therefore their inhibition is expected to result in the suppression of a broad range of downstream pathogenic events [3,5,12,13].

In our attempt to establish a therapy for the polyQ diseases, we hypothesized that molecules that specifically bind to the expanded polyQ stretch would suppress misfolding and aggregation of the expanded polyQ protein. Accordingly, by phage display screening of combinatorial peptide libraries, we identified PolyQ Binding Peptide 1 (QBP1), and proved that QBP1 indeed inhibits polyQ protein misfolding/aggregation *in vitro* [14–16]. Furthermore, we

demonstrated that expression of QBP1 suppresses neurodegeneration *in vivo* in polyQ disease model animals [16,17]. Another approach for targeting misfolding and aggregation of the expanded polyQ protein is to utilize molecular chaperones, which are a group of biomolecules that assist the proper folding of proteins and prevent protein misfolding/aggregation [18–20]. Indeed, overexpression of molecular chaperones such as Hsp40 and Hsp70 has been shown to suppress polyQ protein aggregation and polyQ-induced neurodegeneration in various animal models of the polyQ diseases, such as flies [21–24], worms [25] and mice [26–30]. However, most studies showing the therapeutic efficacy of these aggregation inhibitors have been performed by crossing transgenic animals so far. To develop a therapy using aggregation inhibitors such as QBP1 and molecular chaperones, transgenes need to be delivered in affected individuals by administration, rather than be expressed in the next generation by crossing transgenic animals.

In this study, we employed a viral vector to deliver these transgenes into the brain and investigated their therapeutic effects on polyQ disease model mice. Among various viral vectors, we chose to use adeno-associated virus vector (AAV) because of its widespread infection throughout the brain, its long-term expression of transgenes, and its safety [31,32]. We successfully demonstrate the therapeutic effects of AAV5-QBP1 and AAV5-Hsp40 injections on a mouse model of HD. Most interestingly, we found that AAV5-Hsp40 exerts a non-cell autonomous therapeutic effect, possibly via inhibition of the recently-suggested cell-cell transmission of the polyQ protein, indicating a novel therapeutic mode of action of Hsp40.

## Results

### AAV5-QBP1 and AAV5-Hsp40 Inhibit Inclusion Body Formation in polyQ Disease Mouse Neurons

We employed the R6/2 HD mouse model [33] to investigate the therapeutic effect of AAV-mediated expression of QBP1 and molecular chaperones. We first tested the effect on accumulation of the pathogenic polyQ protein into inclusion bodies in the neurons of R6/2 mice by AAV5 injections. Injections were performed on mice at postnatal day 7 (P7) using an infusion pump (see Materials and Methods), which has been shown to lead to widespread delivery of the injected molecules in the brain [34], and indeed resulted in widespread expression of the transgene throughout the injected brain hemisphere with ~30% infection efficiencies (Fig. S1). R6/2 mice were injected with AAV5-GFP on one side of the striatum and AAV5-QBP1 on the other side, and htt inclusion body formation was compared between the two sides of both the striatum and the cortex. Inclusion bodies were already formed in 36.0% of AAV5-GFP infected neurons in the striatum at 4 weeks of age, which increased to 68.5% at 8 weeks and 73.8% at 14 weeks, and an age dependent increase in inclusion bodies was also observed in the cortex (Fig. S2). In contrast, AAV5-QBP1 infected neurons had significantly less inclusion bodies at most time points (Fig. S2), and the rates of neurons with inclusion bodies at 8 weeks, for example, were 68.5% for GFP vs 33.7% for QBP1 ($p<0.001$) in the striatum, and 49.3% for GFP vs 27.4% for QBP1 ($p<0.001$) in the cortex (Figs. 1A,B). These results demonstrate a significant inhibitory effect of AAV5-QBP1 on inclusion body formation.

We also tested the effect of AAV5-mediated expression of a molecular chaperone on inclusion body formation. Among the various molecular chaperones, we chose to use a member of the Hsp40 family, namely DNAJB1 (referred to as Hsp40 in this study), since members of the DNAJB subfamily have been

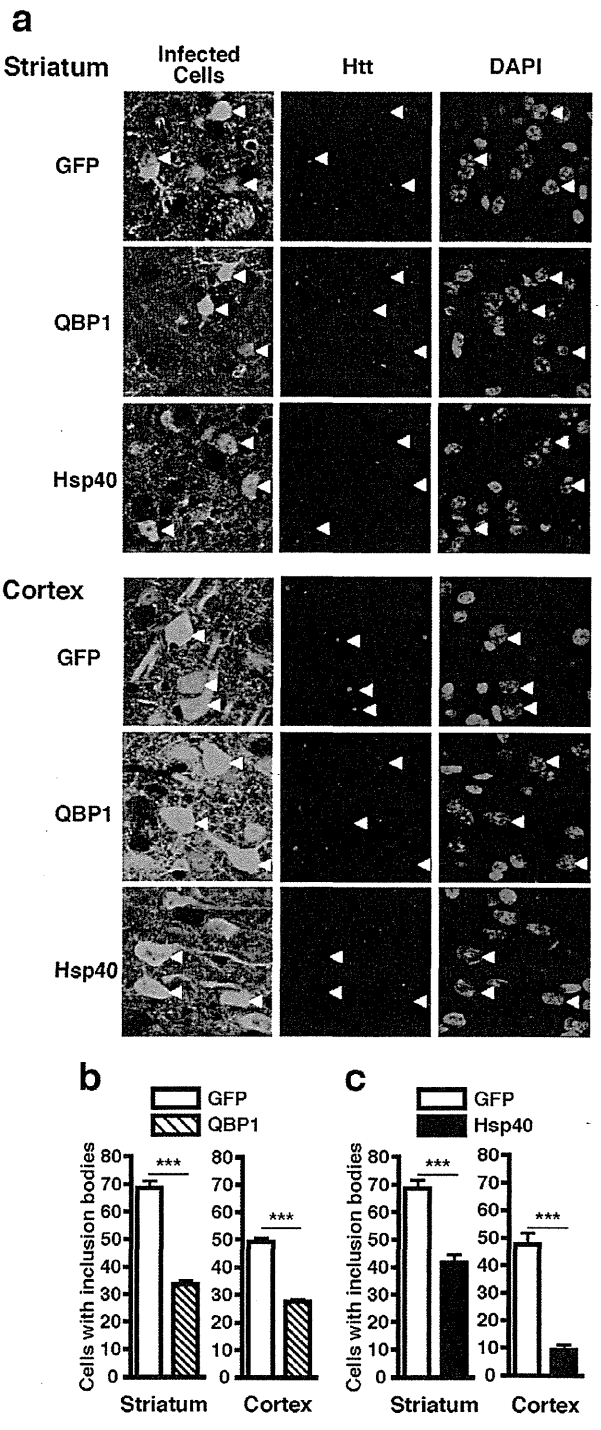


**Figure 1. AAV5-QBP1 and AAV5-Hsp40 inhibit polyQ inclusion body formation in virus infected neurons of polyQ disease mice.** R6/2 mice at P7 were injected with AAV5-GFP on one side of the striatum and either AAV5-QBP1 or AAV5-Hsp40 on the other side, and htt inclusion body formation in virus infected neurons was assessed at 8 weeks of age by immunohistochemistry of brain sections. (A) Representative photographs of striatal (top panels) and cortical (bottom panels) sections of R6/2 mice, injected with the indicated viruses. Green; virus infected cells, red; htt, and blue; nuclei visualized by DAPI staining. In each panel, representative virus infected cells are indicated by white

arrowheads. (B) Inclusion body formation in AAV5-QBP1 infected neurons in the striatum (left) and cortex (right). (C) Inclusion body formation in AAV5-Hsp40 infected neurons in the striatum (left) and cortex (right). In (B) and (C), data are shown as means ± SEM of ≥6 fields of view, in which over 180 cells were counted (*$p<0.05$, ***$p<0.001$). Representative results of two mice analyzed are shown.
doi:10.1371/journal.pone.0051069.g001

reported to be the most potent suppressors of expanded polyQ protein aggregation and toxicity [35]. The effect of AAV5-Hsp40 on polyQ inclusion body formation in R6/2 mice was investigated at 8 weeks, an age at which AAV5-QBP1 showed a clear inhibitory effect. AAV5-Hsp40 also exerted a robust effect on inclusion body formation, and the rates of virus infected neurons with inclusion bodies were 68.6% for GFP vs 41.7% for Hsp40 ($p<0.001$) in the striatum, and 47.5% for GFP vs 9.2% for Hsp40 ($p<0.001$) in the cortex (Figs. 1A,C). This difference in the effectiveness of Hsp40 between the two brain areas may be due to differences in the expression levels of its partner Hsp70. Although whether polyQ inclusion bodies themselves are cytotoxic or cytoprotective has been controversial [36], we assume that suppression of inclusion body formation by QBP1 and Hsp40 can be regarded as a therapeutic effect, since they act by preventing the initial toxic misfolding of the polyQ protein and promoting its refolding, respectively [15,16,19,20]. Therefore, these results collectively demonstrate that QBP1 and Hsp40 exert therapeutic effects in polyQ disease mouse neurons, via their widespread and long-term expression using AAV5.

## AAV5-Hsp40 Improves Neurological Phenotypes of polyQ Disease Mice

Since our above results demonstrated that AAV5-QBP1 and AAV5-Hsp40 inhibit accumulation of the pathogenic polyQ protein into inclusions, we next tested whether this could also lead to amelioration of the neurological phenotypes of R6/2 mice. For this purpose we injected AAV5-GFP, AAV5-QBP1, or AAV5-Hsp40 into both sides of the striatum of P7 R6/2 mice, and analyzed their effects on various neurological phenotypes of these mice.

To evaluate motor impairments of R6/2 mice, we first tested their forced locomotor activity using the rotarod. Although the reduction in rotarod performance of R6/2 mice compared with wild-type (WT) mice becomes evident by 7 weeks of age, the performance of AAV5-QBP1 injected and AAV5-Hsp40 injected R6/2 mice did not significantly differ from AAV5-GFP injected mice (Fig. 2A). We further tested the effect of these viruses on spontaneous locomotor activity. R6/2 mice demonstrated significantly less open-field activity and rearing compared with WT mice as early as 5 weeks of age, which further decreased by 8 weeks. Although we could not detect a significant improvement in AAV5-QBP1 injected mice, AAV5-Hsp40 injected R6/2 mice exhibited significantly higher open-field activity and rearing compared with AAV5-GFP injected mice at 8 weeks of age (Activity: GFP 134.8±10.2 vs Hsp40 196.4±8.4 counts/min, $p<0.001$; Rearing: GFP 2.0±0.44 vs<Hsp40 6.3±0.67 counts/min, $p<0.001$) (Figs. 2B,C). These results demonstrate the therapeutic effect of AAV5-Hsp40 on the decreased spontaneous locomotor activity of R6/2 mice.

We also tested the effect of each virus on the grip strength abnormality of R6/2 mice. Grip strength of R6/2 mice was significantly weaker than that of WT mice at 9 weeks of age, and further weakened by 12 weeks of age. AAV5-QBP1 injection did not have a significant effect on grip strength at either age. In contrast, AAV5-Hsp40 injected R6/2 mice exhibited significantly

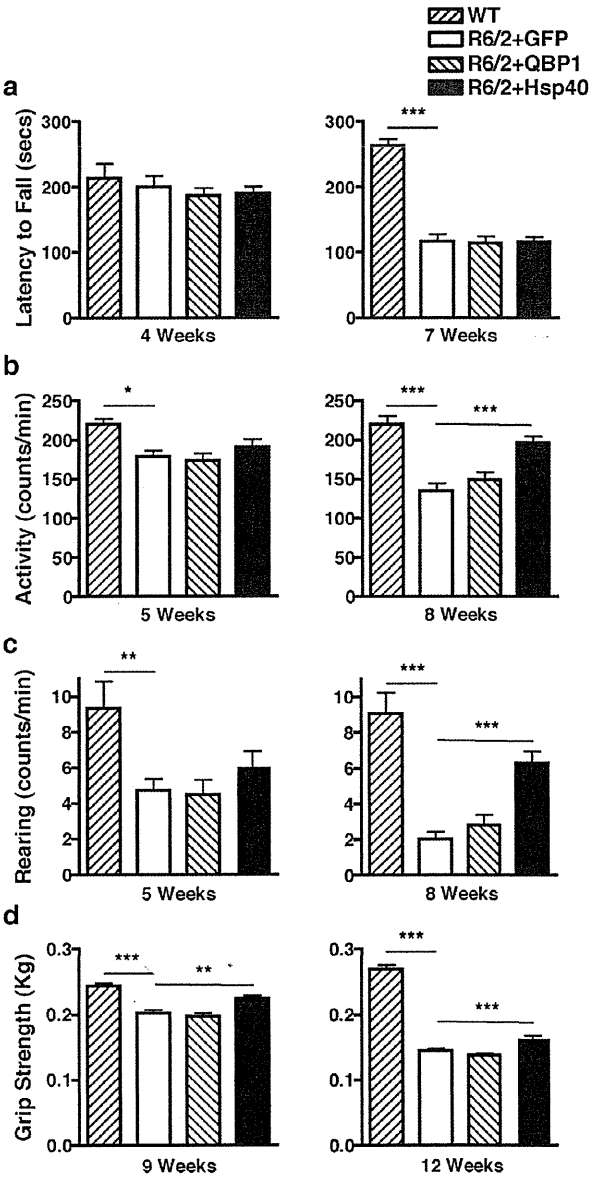


**Figure 2. AAV5-Hsp40 improves spontaneous locomotor activity and grip strength abnormalities of polyQ disease mice.** R6/2 mice at P7 were injected in both sides of the striatum with AAV5-GFP, AAV5-QBP1, or AAV5-Hsp40, and the following phenotypes were analyzed. (A) Rotarod performance measured at 4 (left) and 7 weeks (right) of age. (B, C) Open-field activity (B) and rearing (C) measured at 5 (left) and 8 weeks (right) of age. (D) Grip strength measured at 9 (left) and 12 weeks (right) of age. Values represent mean ± SEM, n≥9 mice (*$p<0.05$, **$p<0.01$, ***$p<0.001$).
doi:10.1371/journal.pone.0051069.g002

greater grip strengths than AAV5-GFP injected mice both at 9 weeks (GFP 0.202±0.005 vs Hsp40 0.225±0.005 Kg, $p<0.01$) and 12 weeks of age (GFP 0.145±0.003 vs Hsp40 0.165±0.003 Kg, $p<0.001$), demonstrating the therapeutic effect of AAV5-Hsp40 (Fig. 2D).

We also evaluated the body weight loss of AAV5-injected R6/2 mice. AAV5-GFP injected R6/2 mice demonstrated significantly lower body weights than WT mice after 9 weeks of age. The

weights of AAV5-QBP1 injected R6/2 mice were almost indistinguishable from AAV5-GFP injected mice at each time point. In contrast, the weights of AAV5-Hsp40 injected R6/2 mice showed a significant improvement compared to AAV5-GFP injected mice between 9 and 13 weeks of age (Fig. 3A). These results demonstrate the therapeutic effect of AAV5-Hsp40 also against the weight loss of R6/2 mice.

We then assessed the effect of AAV5 injections on the lifespan of R6/2 mice. The survival of AAV5-QBP1 injected R6/2 mice (median lifespan 100 days) was not significantly different from AAV5-GFP injected mice (median lifespan 95 days). In contrast, AAV5-Hsp40 injection resulted in a rightward shift of the survival curve to a median lifespan of 112 days, demonstrating the therapeutic effect of AAV5-Hsp40 on the decreased survival of R6/2 mice (Fig. 3B). Taken together, these results clearly demonstrate that AAV5-Hsp40 significantly improves many neurological phenotypes of R6/2 mice.

## AAV5-Hsp40 Inhibits Inclusion Body Formation also in Virus Non-infected Neurons of polyQ Disease Mice

When analyzing the effect of the viruses on inclusion body formation in R6/2 mice (Fig. 1), we suspected that on the AAV5-Hsp40 injected side, not only virus infected neurons, but even virus non-infected neurons appeared to have fewer inclusion bodies than those on the AAV5-GFP injected side. To clarify our suspicion, we focused on the virus non-infected neurons that are not stained with Hsp40 or GFP antibodies (see Materials and Methods and Fig. S3), and reanalyzed inclusion body formation in the virus non-infected neurons. On the AAV5-QBP1 injected side, virus non-infected neurons showed a similar rate of inclusion body formation as non-infected neurons on the AAV5-GFP injected side, in both the striatum and cortex, as expected (Fig. 4). Surprisingly, we found that on the AAV5-Hsp40 injected side, virus non-infected neurons had strikingly fewer inclusion bodies compared with non-infected neurons on the AAV5-GFP injected side in both the striatum (GFP side 69.0% vs Hsp40 side 49.8%, $p<0.01$) and cortex (GFP side 59.1% vs Hsp40 side 39.6%,

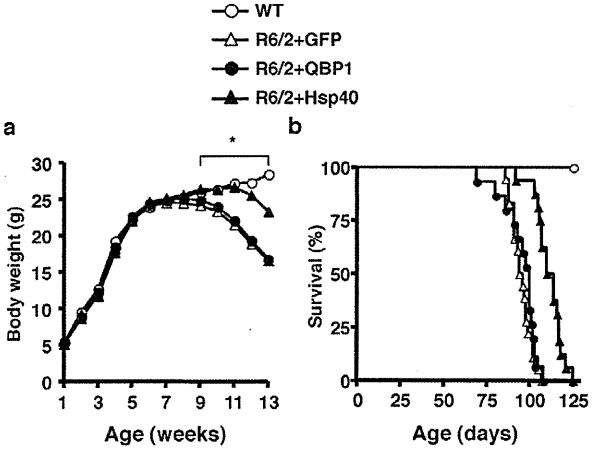


**Figure 3. AAV5-Hsp40 improves body weight loss and extends the lifespan of polyQ disease mice.** R6/2 mice at P7 were injected in both sides of the striatum with AAV5-GFP, AAV5-QBP1, or AAV5-Hsp40, and the following phenotypes were analyzed. (A) Body weight measured weekly. Values represent the mean (*$p<0.05$, R6/2+GFP vs R6/2+Hsp40). (B) Survival ($p<0.0001$, R6/2+GFP vs R6/2+Hsp40, Log-rank test). In both (A) and (B), n≥9 mice.
doi:10.1371/journal.pone.0051069.g003

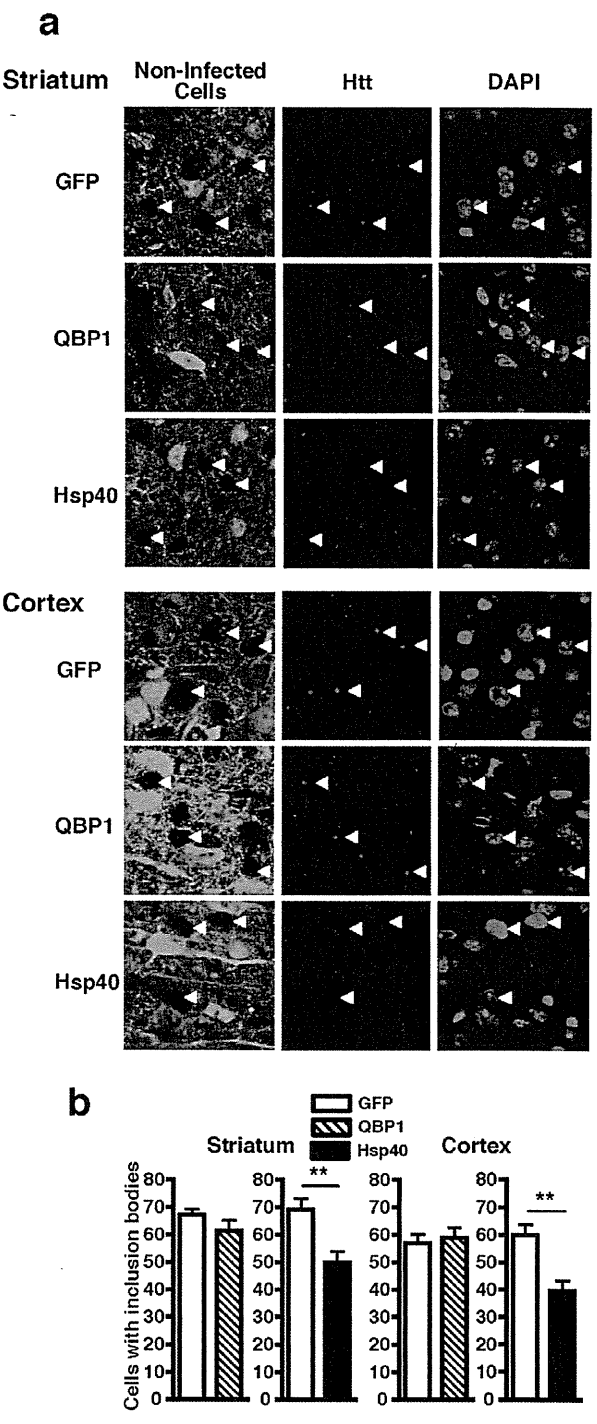


**Figure 4. AAV5-Hsp40 also inhibits polyQ inclusion body formation in virus non-infected neurons of polyQ disease mouse brains.** Htt inclusion body formation in 8 week old R6/2 mouse brains injected with AAV5-GFP on one side of the striatum and AAV5-QBP1 or AAV5-Hsp40 on the other side, was analyzed as in Fig. 1, but in the virus non-infected cells on each side of the brain. (A) Representative photographs of striatal (top panels) and cortical (bottom panels) sections of R6/2 mice injected with the indicated viruses. Green; virus infected cells, red; htt, and blue; nuclei visualized by DAPI staining. Representative virus non-infected cells in each panel are indicated by

white arrowheads. (B) Inclusion body formation in virus non-infected cells on the AAV5-QBP1 injected side and AAV5-Hsp40 injected side in the striatum (left) and cortex (right). Data are shown as means ± SEM of ≥6 fields of view, in which over 180 cells were counted (**$p<0.01$). Representative results of two mice analyzed are shown.
doi:10.1371/journal.pone.0051069.g004

$p<0.01$). The degree of inhibition was not as robust as in AAV5-Hsp40 infected neurons, but was still significant. These results raise a possibility that Hsp40 can exert a non-cell autonomous therapeutic effect on virus non-infected neurons in the brains of R6/2 mice, which is not observed with QBP1.

### Hsp40 Inhibits Secretion of Pathogenic polyQ Proteins from Cultured Cells

We next aimed to elucidate the mechanism by which Hsp40 exerts its non-cell autonomous therapeutic effect in the brains of R6/2 mice. Recent studies suggest that prion-like cell-cell transmission of aggregation-prone proteins via their release from cells and subsequent uptake into neighboring cells, is involved in the spreading of neuropathology in the polyQ diseases as well as other neurodegenerative diseases [8–11]. We therefore hypothesized that Hsp40 may inhibit secretion of the pathogenic polyQ protein from cells to exert its non-cell autonomous therapeutic effect.

We used a cell culture model to test whether Hsp40 could inhibit secretion of a pathogenic polyQ protein from cells. An expanded polyQ stretch of 81 repeats fused with CFP and a V5 tag (Q81-CFP-V5) was co-expressed together with the GFP control, QBP1, or Hsp40 in Neuro2A cells. Twenty-four h later, the culture media were replaced with fresh media to remove all of the dead cells, and after a further 6 h of incubation, culture media were collected and concentrated using centrifugal filters, and subjected to Western blot analysis. Q81-CFP-V5 was detected in the culture medium of cells (Fig. 5A), suggesting that pathogenic polyQ proteins are secreted from cells. In cells co-expressing QBP1, the amount of Q81-CFP-V5 detected in the culture medium was similar to that in cells co-expressing GFP. In contrast, Neuro2A cells co-expressing Hsp40 showed ~40% less Q81-CFP-V5 in the culture medium compared with cells co-expressing GFP, suggesting that Hsp40 inhibits secretion of the pathogenic polyQ protein from cells (Figs. 5A,B). Furthermore, siRNA-mediated knockdown of endogenous Hsp40 increased the secretion of Q81-CFP-V5 by ~40% compared with cells treated with a control siRNA (Figs. 5C,D), indeed confirming that Hsp40 inhibits polyQ protein secretion. These results imply that inhibition of secretion of the polyQ protein from cells by Hsp40 results in a non cell-autonomous therapeutic effect in R6/2 mouse brains, possibly via inhibition of the cell-cell transmission of the pathogenic polyQ protein.

## Discussion

In this study we show for the first time that viral vector-mediated expression of a molecular chaperone, namely Hsp40 significantly improves the neurological phenotypes of a mouse model of the polyQ diseases. Although a recent study reported the effectiveness of another Hsp40 family member, HSJ1a (DNAJB2a) in R6/2 mice, this study cannot be directly translated to a therapy since it was performed by the crossing of transgenic mice [30]. In addition, although lentiviral vector-mediated delivery of DNAJB2a to a polyQ disease rat model has been investigated [37], it did not demonstrate the therapeutic effect on the neurological phenotypes, perhaps because of the limited spread of lentiviruses. We successfully overcame these above problems by using AAV, which infects a widespread area of the brain, and is already used in human patients [38].

We did not detect significant therapeutic effects of AAV5-Hsp70 on R6/2 mice unlike AAV5-Hsp40, possibly due to the very low infection rate of our AAV5-Hsp70 (data not shown), or differences in the effectiveness of Hsp40 and Hsp70 against mutant htt. Indeed, previous studies examining the effect of Hsp70 in R6/2 mice have shown no or very modest therapeutic effects [28,29]. Furthermore, a cell culture study demonstrated that Hsp40 family members are effective against the toxicity of mutant htt, while Hsp70 family members are ineffective [35]. Taken together, these studies indicate that Hsp40 family members may be more effective than Hsp70 family members against the toxic effects of mutant htt.

We surprisingly found that AAV5-Hsp40 inhibits inclusion body formation also in virus non-infected cells (Fig. 4), suggesting a non cell-autonomous therapeutic effect. Aggregation prone proteins that cause neurodegenerative diseases including pathogenic polyQ proteins, as well as α-synuclein which causes Parkinson's disease, and tau which causes the tauopathies have recently been suggested to be transmitted between cells, and this may be the mechanism leading to the progressive spread of neuropathology in these diseases [8–11]. We detected a significant amount of the pathogenic polyQ protein in the culture medium of Neuro2A cells (Fig. 5A), suggesting its cell-cell transmission, which is compatible with previous studies [39,40]. We further found that Hsp40 suppresses secretion of the pathogenic polyQ protein from cells (Fig. 5), suggesting that it may inhibit the cell-cell transmission of the pathogenic polyQ protein. The non-cell autonomous therapeutic effect of Hsp40 may also involve other mechanisms, such as (1) AAV5-Hsp40 infected neurons may create a better environment for contacting non-infected neurons [41] or (2) Hsp40 itself may be secreted to exert therapeutic effects on neighboring non-infected neurons, as is suggested for Hsp70 [42].

We were unable to detect the therapeutic effect of AAV5-QBP1 on the neurological phenotypes of R6/2 mice, although we successfully detected its inhibition of inclusion body formation. However, we and others have previously shown that expression of QBP1 exerts therapeutic effects on the neurological phenotypes of *Drosophila* and mouse models of the polyQ diseases [16,17,43]. Since the infection efficiency of all of the viruses used in this study was quite low (~30%), the extent of neurons expressing QBP1 in the R6/2 mouse brains was probably insufficient to exert a detectable effect on the phenotypes. On the other hand, in the case of AAV5-Hsp40, inhibition of polyQ protein secretion which should lead to an increase in the number of rescued neurons, likely contributed to its improvement of the neurological phenotypes. Other possibilities may also contribute to their varying effects, for example (1) Hsp40 is more effective than QBP1 in inhibiting polyQ protein misfolding/aggregation, and (2) Hsp40 can also support the degradation of misfolded proteins [19], while QBP1 cannot.

In this study we demonstrate a therapeutic strategy against the polyQ diseases using AAV5-Hsp40, which has great potential for clinical application, since AAVs are safe and are widely utilized in clinical trials [38]. We further suggest a novel therapeutic mode of action of Hsp40, namely suppression of pathogenic polyQ protein secretion from cells, which may consequently suppress its cell-cell transmission. Since the transmission of aggregation-prone proteins is thought to be involved also in other neurodegenerative diseases, Hsp40 may exert a non-cell autonomous therapeutic effect on these other diseases. Elucidation of how Hsp40 inhibits polyQ protein secretion should reveal new therapeutic targets and

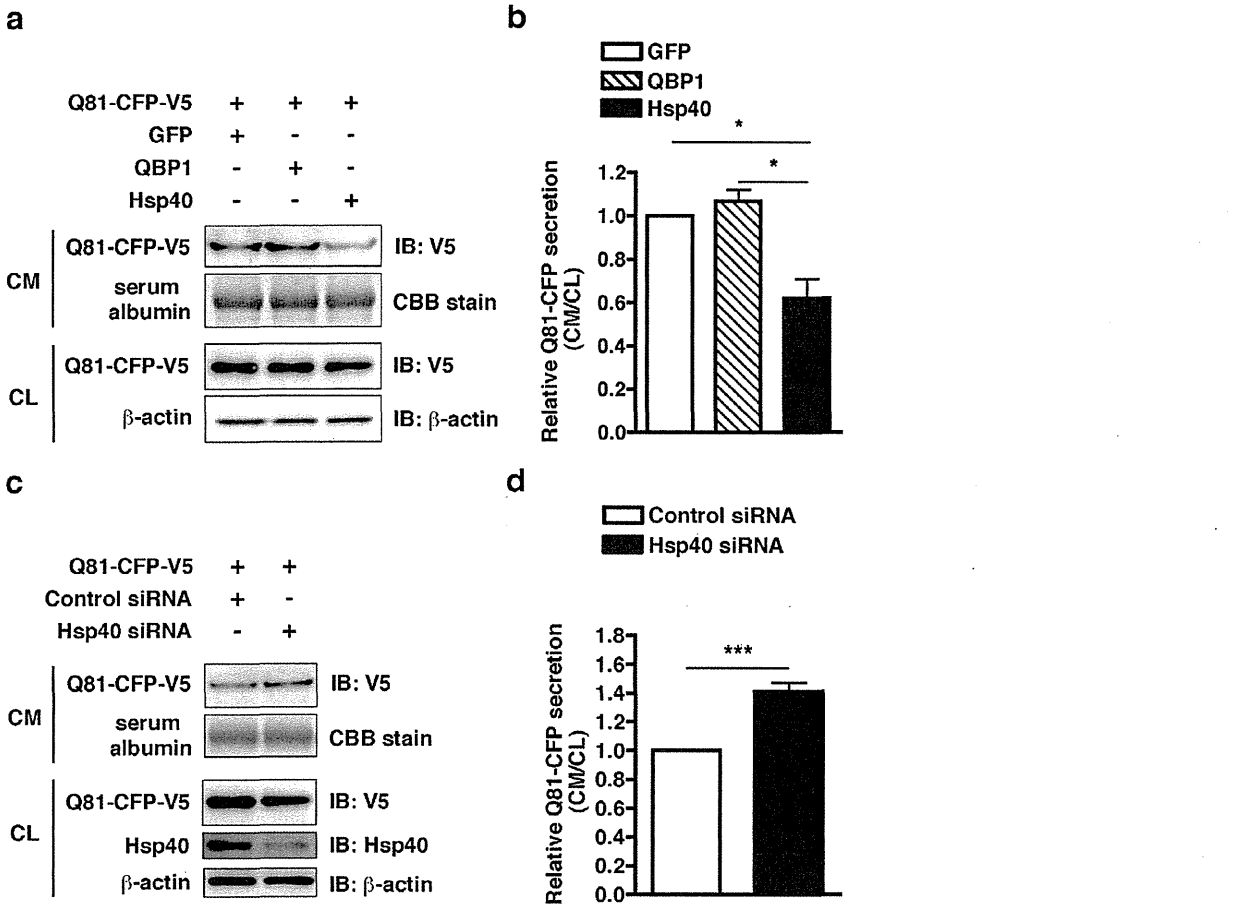


**Figure 5. Hsp40 inhibits polyQ protein secretion in cultured cells.** (A) Neuro2A cells were co-transfected with plasmids expressing Q81-CFP-V5 and either GFP, QBP1, or Hsp40, and the culture media (CM) and cell lysates (CL) were subjected to Western blot analysis with a V5 antibody to detect the Q81-CFP-V5 protein. (B) Relative amounts of Q81-CFP-V5 secreted into the culture media, calculated from the band intensities in (A), with the amount of Q81-CFP-V5 secreted from cells co-expressing GFP set to 1. (C) Neuro2A cells were transfected with a plasmid expressing Q81-CFP-V5 and siRNA against Hsp40 or a control siRNA, and the culture media (CM) and cell lysates (CL) were subjected to Western blot analysis with a V5 antibody to detect the Q81-CFP-V5 protein, and with an Hsp40 antibody. The loading controls are as in (A). (D) Relative amounts of Q81-CFP-V5 secreted into the cuture media, calculated from the band intensities in (C). In (A) and (C), serum albumin is shown as a loading control for the culture media, and β-actin as a loading control for the cell lysates. In (B) and (D), data are shown as means ± SEM of ≥ four independent experiments (*$p<0.05$, ***$p<0.001$).
doi:10.1371/journal.pone.0051069.g005

strategies for neurodegenerative diseases caused by aggregation-prone proteins.

## Materials and Methods

### Viral Vectors

Adeno-associated virus type 5 (AAV5) vector plasmids contained an expression cassette with a human cytomegalovirus enhancer/chicken β actin (CAG) promoter followed by the first intron of human growth hormone, target cDNA (either a tandem repeat of QBP1 fused to GFP [14], human Hsp40 (DNAJB1) [44], or GFP), and a simian virus 40 polyadenylation signal sequence, all positioned between the inverted terminal repeats of the AAV5 genome. AAV5 vectors were produced using the AAV5 plasmid, the AAV5 helper plasmid containing the rep and cap sequences from AAV5, as well as the pHelper plasmid from the AAV Helper-Free System containing the E2A, E4, and VA RNA genes of the adenovirus genome (Stratagene, La Jolla, CA). HEK293 cells were co-transfected with the AAV5 plasmid and two helper plasmids by the calcium phosphate method. Seventy-two h later, the cells were harvested and subjected to three rounds of freeze-thaw lysis. AAV5 vectors were then purified by two rounds of cesium chloride density gradient centrifugation. Vector titers were estimated by quantitative DNA dot-blot hybridization to be ~$0.2–1.6\times10^{13}$ genome copies/ml.

### Animals

All animal experiments were performed in accordance with the guidelines of the Animal Ethics Committee of the National Institute of Neuroscience, National Center of Neurology and Psychiatry, Japan, and performed in accordance with the guidelines. Mice transgenic for human *huntingtin* exon 1 with approximately 150 CAG repeats (strain R6/2) [33] were obtained from the Jackson Laboratory (Bar Harbor, ME), and maintained on a B6CBAF1 background. Genotypes were analyzed and CAG repeat numbers of the transgenic mice were confirmed to be

similar by PCR as previously described [33]. Mice were housed on a 12-hour light/dark cycle, with food and water provided *ad libitum*. At least nine male R6/2 mice per group and wild-type littermate (WT) controls were used for the phenotype analyses, and two R6/2 mice were used for the inclusion body analyses.

## AAV Injections

P7 old R6/2 mice were stereotaxically injected with 1 µl of virus solution (AAV5-GFP, AAV5-QBP1, or AAV5-Hsp40) into the striatum (coordinates 1 mm anterior to bregma, 2.25 mm lateral to the midline, and 3 mm ventral to the skull surface) at a rate of 0.1 µl/min using a 10 µl Hamilton syringe (Hamilton Company, Reno, NV) and an infusion pump (KD Scientific, Holliston, MA). For inclusion body analyses, AAV5-GFP was injected into one side of the striatum and AAV5-QBP1 or AAV5-Hsp40 into the other side. For phenotype analyses, the same virus was injected into both sides of the striatum.

## Mouse Phenotype Analyses

For rotarod analysis, mice were tested at 4 and 7 weeks of age on an accelerating rotarod apparatus (Ugo Basile, Comerio, Italy) set to accelerate from 4 to 40 rpm over a period of 300 seconds. The time it took for each mouse to either fall off the rod or cling onto the rod for one full rotation was recorded. Mice were tested on the rod for three consecutive days, with three trials per day. The first day was regarded as training, and only the data from the second and third day were used. The highest and lowest values were excluded, and the middle four values were averaged. Grip strength analysis was performed at 9 and 12 weeks of age using a grip strength meter (Muromachi Kikai, Tokyo, Japan). Mice were placed gently by their tail on the metal grid of the meter so that they grip the grid with both forelimbs and hindlimbs, at which point they were pulled back gently with their tails, exerting a tension that is measured by the meter. Five trials were performed for each mouse, and the highest and lowest values were excluded and the middle three values were averaged. To measure open-field activity and rearing, mice at 5 and 8 weeks of age were tested using a spontaneous locomotor activity monitor (Supermex, Muromachi Kikai, Tokyo, Japan), consisting of an acrylic box of dimensions 40 cm×28 cm×31 cm with an activity sensor placed at the top and rearing sensors placed at the sides of the box. Mice were left in the box for a total of 15 min, and their activity count and rearing frequency were measured. For body weight analysis mice were weighed weekly. Mice were followed until their deaths in order to calculate their lifespans, a widely accepted and valuable parameter to assess therapeutic effects in these mice, which was approved by the institution's Animal Ethics Committee.

## Tissue Preparation and Immunohistochemical Analyses

Mice were deeply anesthetized with sodium pentobarbital (100 mg/kg), and then perfused intercardially with saline followed by 4% paraformaldehyde (PFA) in phosphate-buffered saline (PBS). Brains were removed, post-fixed in 4% PFA in PBS at 4°C overnight, and then cryoprotected in 30% sucrose in PBS at 4°C for 24 h. Frozen 10 µm sections were cut using a cryostat. For immunohistochemical analysis, sections were blocked in PBS containing 5% goat serum and 0.1% Triton X-100 for 1 h at room temperature. The sections were then incubated with a mouse anti-huntingtin antibody (1:250; MAB5374, Millipore, Billerica, MA), and either a rabbit anti-Hsp40 antibody (1:500; SPA-400, Enzo Life Sciences, Farmingdale, NY) or a rabbit anti-GFP antibody (1:250; A11122, Invitrogen, Carlsbad, CA) at 4°C overnight, followed by an Alexa Fluor 596-conjugated goat anti-mouse IgG antibody and an Alexa Fluor 488 goat anti-rabbit IgG antibody (1:1000, Invitrogen) for 1 h at room temperature. Sections were mounted with Slowfade Gold antifade reagent with DAPI (Invitrogen) and examined using a confocal laser scanning microscope (FV1000; Olympus, Tokyo, Japan). The average fluorescence intensity of representative cells that were regarded as either "infected" or "non-infected" in each sample were measured using the Image J software, confirming that the two population of cells can readily be distinguished in the images (Fig. S3).

## Cell Culture, Transfection and Western Blot Analysis

Neuro2A cells (obtained from ATCC) were grown and maintained in DMEM supplemented with 10% (v/v) FBS. Cells were plated on a 35-mm dish at a density of $4\times10^5$ cells per dish on the day before transfection. For the overexpression experiment, a plasmid vector encoding a tandem repeat of QBP1 fused to GFP, human Hsp40 [44], or GFP was transiently co-transfected with the Q81-CFP-V5 vector encoding an expanded polyQ stretch of 81 repeats fused with CFP and a V5 tag, using Lipofectamine LTX with PLUS reagent (Invitrogen). For the knockdown experiment, siRNA targeted against mouse Hsp40 (Santa Cruz Biotechnology, Santa Cruz, CA) or a control siRNA (RNAi Inc, Tokyo, Japan) was cotransfected with the Q81-CFP-V5 vector using Lipofectamine 2000 reagent (Invitrogen). At 24 h after transfection, culture media were replaced with fresh media, and after a further 6 h of incubation, culture media were collected and whole cell lysates were prepared with 1% Triton X in tris-buffered saline. For Western blot analysis, the culture media were concentrated using 30 kDa cutoff Amicon Ultra filters (Millipore). Q81-CFP-V5 in the concentrated culture media and whole cell lysates was separated using 10% SDS-PAGE gels and transferred onto PVDF membranes (Bio-Rad, Hercules, CA). The membranes were incubated overnight with an HRP-conjugated anti-V5 antibody (1:2500, Invitrogen) at 4°C. The HRP signal was visualized with SuperSignal West Femto Chemiluminescent Substrate (Thermo Fisher Scientific Inc, Rockford, IL), captured with a LAS-3000 mini CCD imaging system (Fujifilm, Tokyo, Japan), and band intensities were quantified using the Image J software. For the siRNA experiments, the membranes were then stripped and incubated with a rabbit anti-Hsp40 antibody (1:5000, SPA-400, Enzo Life Sciences Inc, Farmingdale, NY) at 4°C followed by an HRP-conjugated anti-rabbit IgG secondary antibody (1:10000, Thermo Fisher Scientific), and visualized as above.

## Statistical Analyses

For the rotarod, open-field activity, rearing, grip strength and weight data, statistical analyses were performed by using one-way analysis of variance followed by Tukey's multiple comparison test to assess for significant differences between individual groups. The survival data was analyzed using the Log-rank test. For the inclusion body formation and Western blot analyses, Student's *t*-test was used. For all analyses, $p<0.05$ was considered as significant.

# Supporting Information

**Figure S1 AAV5 injection into the mouse striatum at P7 results in widespread expression of the transgene.** R6/2 mice at P7 were injected in the right striatum with 1 µl of AAV5-QBP1, and 2 weeks later the expression of QBP1 was analyzed by immunohistochemistry. This widespread expression of QBP1 throughout the brain lasts for at least 13 weeks (data not shown). (PDF)

**Figure S2 AAV5-QBP1 inhibits polyQ inclusion body formation in virus infected neurons of polyQ disease**

**mice.** R6/2 mice at P7 were injected with AAV5-GFP on one side of the striatum and AAV5-QBP1 on the other side, and at 4, 8, and 14 weeks of age htt inclusion body formation in virus infected neurons of the striatum (left) and cortex (right) was assessed by immunohistochemistry. Data are shown as means ± SEM of ≥ 6 fields of view, in which over 180 cells were counted (*$p<0.05$, ***$p<0.001$). Representative results of two mice analyzed are shown.
(PDF)

**Figure S3 AAV5 "infected" and "non-infected" cells can be clearly distinguished from their fluorescence intensity.** The fluorescence intensity of representative cells that were regarded as either "infected" or "non-infected" in photographs of immunostained brain sections of R6/2 mice injected with either AAV5-GFP (left), AAV5-QBP1 (middle) or AAV5-Hsp40 (right). For each sample, a total of over 100 representative cells were analyzed from 5–6 fields of view.
(PDF)

## Acknowledgments

We thank Kenzo Ohtsuka for the human Hsp40 cDNA, Yoshinaga Saeki and Hirokazu Hirai for helpful discussions, and Reiko Sasaki, Hirokazu Matsushima, Naomi Takino, Hitomi Miyauchi, and Keiko Ayabe for their technical assistance.

## Author Contributions

Conceived and designed the experiments: HAP T. Takeuchi SM T. Toda KW YN. Performed the experiments: HAP T. Takeuchi HF KY CI HY. Analyzed the data: HAP T. Takeuchi T. Toda KW YN. Contributed reagents/materials/analysis tools: SM. Wrote the paper: HAP T. Takeuchi YN.

## References

1. Gusella JF, MacDonald ME (2000) Molecular genetics: unmasking polyglutamine triggers in neurodegenerative disease. Nat Rev Neurosci 1: 109–115.
2. Orr HT, Zoghbi HY (2007) Trinucleotide repeat disorders. Annu Rev Neurosci 30: 575–621.
3. Michalik A, Van Broeckhoven C (2003) Pathogenesis of polyglutamine disorders: aggregation revisited. Hum Mol Genet 12 Spec No2: R173–186.
4. Shao J, Diamond MI (2007) Polyglutamine diseases: emerging concepts in pathogenesis and therapy. Hum Mol Genet 16 Spec No.2: R115–123.
5. Nagai Y, Popiel HA (2008) Conformational changes and aggregation of expanded polyglutamine proteins as therapeutic targets of the polyglutamine diseases: exposed β-sheet hypothesis. Curr Pharm Des 14: 3267–3279.
6. Williams AJ, Paulson HL (2008) Polyglutamine neurodegeneration: protein misfolding revisited. Trends Neurosci 31: 521–528.
7. Bauer PO, Nukina N (2009) The pathogenic mechanisms of polyglutamine diseases and current therapeutic strategies. J Neurochem 110: 1737–1765.
8. Aguzzi A, Rajendran L (2009) The transcellular spread of cytosolic amyloids, prions, and prionoids. Neuron 64: 783–790.
9. Brundin P, Melki R, Kopito R (2010) Prion-like transmission of protein aggregates in neurodegenerative diseases. Nat Rev Mol Cell Biol 11: 301–307.
10. Lee SJ, Desplats P, Sigurdson C, Tsigelny I, Masliah E (2010) Cell-to-cell transmission of non-prion protein aggregates. Nat Rev Neurol 6: 702–706.
11. Frost B, Diamond MI (2010) Prion-like mechanisms in neurodegenerative diseases. Nat Rev Neurosci 11: 155–159.
12. Bates G (2003) Huntingtin aggregation and toxicity in Huntington's disease. Lancet 361: 1642–1644.
13. Herbst M, Wanker EE (2006) Therapeutic approaches to polyglutamine diseases: combating protein misfolding and aggregation. Curr Pharm Des 12: 2543–2555.
14. Nagai Y, Tucker T, Ren H, Kenan DJ, Henderson BS, et al. (2000) Inhibition of polyglutamine protein aggregation and cell death by novel peptides identified by phage display screening. J Biol Chem 275: 10437–10442.
15. Nagai Y, Inui T, Popiel HA, Fujikake N, Hasegawa K, et al. (2007) A toxic monomeric conformer of the polyglutamine protein. Nat Struct Mol Biol 14: 332–340.
16. Popiel HA, Burke JR, Strittmatter WJ, Oishi S, Fujii N, et al. (2011) The aggregation inhibitor peptide QBP1 as a therapeutic molecule for the polyglutamine neurodegenerative diseases. J Amino Acids 2011: 265084.
17. Nagai Y, Fujikake N, Ohno K, Higashiyama H, Popiel HA, et al. (2003) Prevention of polyglutamine oligomerization and neurodegeneration by the peptide inhibitor QBP1 in *Drosophila*. Hum Mol Genet 12: 1253–1259.
18. Liberek K, Lewandowska A, Zietkiewicz S (2008) Chaperones in control of protein disaggregation. EMBO J 27: 328–335.
19. Kampinga HH, Craig EA (2010) The HSP70 chaperone machinery: J proteins as drivers of functional specificity. Nat Rev Mol Cell Biol 11: 579–592.
20. Hartl FU, Bracher A, Hayer-Hartl M (2011) Molecular chaperones in protein folding and proteostasis. Nature 475: 324–332.
21. Warrick JM, Chan HY, Gray-Board GL, Chai Y, Paulson HL, et al. (1999) Suppression of polyglutamine-mediated neurodegeneration in *Drosophila* by the molecular chaperone HSP70. Nat Genet 23: 425–428.
22. Kazemi-Esfarjani P, Benzer S (2000) Genetic suppression of polyglutamine toxicity in *Drosophila*. Science 287: 1837–1840.
23. Fernandez-Funez P, Nino-Rosales ML, de Gouyon B, She WC, Luchak JM, et al. (2000) Identification of genes that modify ataxin-1-induced neurodegeneration. Nature 408: 101–106.
24. Chan HY, Warrick JM, Gray-Board GL, Paulson HL, Bonini NM (2000) Mechanisms of chaperone suppression of polyglutamine disease: selectivity, synergy and modulation of protein solubility in *Drosophila*. Hum Mol Genet 9: 2811–2820.
25. Satyal SH, Schmidt E, Kitagawa K, Sondheimer N, Lindquist S, et al. (2000) Polyglutamine aggregates alter protein folding homeostasis in *Caenorhabditis elegans*. Proc Natl Acad Sci USA 97: 5750–5755.
26. Cummings CJ, Sun Y, Opal P, Antalffy B, Mestril R, et al. (2001) Over-expression of inducible HSP70 chaperone suppresses neuropathology and improves motor function in SCA1 mice. Hum Mol Genet 10: 1511–1518.
27. Adachi H, Katsuno M, Minamiyama M, Sang C, Pagoulatos G, et al. (2003) Heat shock protein 70 chaperone overexpression ameliorates phenotypes of the spinal and bulbar muscular atrophy transgenic mouse model by reducing nuclear-localized mutant androgen receptor protein. J Neurosci 23: 2203–2211.
28. Hansson O, Nylandsted J, Castilho RF, Leist M, Jaattela M, et al. (2003) Overexpression of heat shock protein 70 in R6/2 Huntington's disease mice has only modest effects on disease progression. Brain Res 970: 47–57.
29. Hay DG, Sathasivam K, Tobaben S, Stahl B, Marber M, et al. (2004) Progressive decrease in chaperone protein levels in a mouse model of Huntington's disease and induction of stress proteins as a therapeutic approach. Hum Mol Genet 13: 1389–1405.
30. Labbadia J, Novoselov SS, Bett JS, Weiss A, Paganetti P, et al. (2012) Suppression of protein aggregation by chaperone modification of high molecular weight complexes. Brain.
31. Okada T, Nomoto T, Shimazaki K, Lijun W, Lu Y, et al. (2002) Adeno-associated virus vectors for gene transfer to the brain. Methods 28: 237–247.
32. Davidson BL, Breakefield XO (2003) Viral vectors for gene delivery to the nervous system. Nat Rev Neurosci 4: 353–364.
33. Mangiarini L, Sathasivam K, Seller M, Cozens B, Harper A, et al. (1996) Exon 1 of the HD gene with an expanded CAG repeat is sufficient to cause a progressive neurological phenotype in transgenic mice. Cell 87: 493–506.
34. Bobo RH, Laske DW, Akbasak A, Morrison PF, Dedrick RL, et al. (1994) Convection-enhanced delivery of macromolecules in the brain. Proc Natl Acad Sci USA 91: 2076–2080.
35. Hageman J, Rujano MA, van Waarde MA, Kakkar V, Dirks RP, et al. (2010) A DNAJB chaperone subfamily with HDAC-dependent activities suppresses toxic protein aggregation. Mol Cell 37: 355–369.
36. Ross CA, Poirier MA (2005) Opinion: What is the role of protein aggregation in neurodegeneration? Nat Rev Mol Cell Biol 6: 891–898.
37. Howarth JL, Kelly S, Keasey MP, Glover CP, Lee YB, et al. (2007) Hsp40 molecules that target to the ubiquitin-proteasome system decrease inclusion formation in models of polyglutamine disease. Mol Ther 15: 1100–1105.
38. Muramatsu S, Fujimoto K, Kato S, Mizukami H, Asari S, et al. (2010) A phase I study of aromatic L-amino acid decarboxylase gene therapy for Parkinson's disease. Mol Ther 18: 1731–1735.
39. Ren PH, Lauckner JE, Kachirskaia I, Heuser JE, Melki R, et al. (2009) Cytoplasmic penetration and persistent infection of mammalian cells by polyglutamine aggregates. Nat Cell Biol 11: 219–225.
40. Herrera F, Tenreiro S, Miller-Fleming L, Outeiro TF (2011) Visualization of cell-to-cell transmission of mutant huntingtin oligomers. PLoS Curr 3: RRN1210.
41. Goodenough DA, Paul DL (2009) Gap junctions. Cold Spring Harb Perspect Biol 1: a002576.
42. Calderwood SK, Mambula SS, Gray PJ, Jr., Theriault JR (2007) Extracellular heat shock proteins in cell signaling. FEBS Lett 581: 3689–3694.
43. Bauer PO, Goswami A, Wong HK, Okuno M, Kurosawa M, et al. (2010) Harnessing chaperone-mediated autophagy for the selective degradation of mutant huntingtin protein. Nat Biotechnol 28: 256–263.
44. Ohtsuka K (1993) Cloning of a cDNA for heat-shock protein hsp40, a human homologue of bacterial DnaJ. Biochem Biophys Res Commun 197: 235–240.

HMG Advance Access published April 14, 2013

*Human Molecular Genetics, 2013* *1–13*
*doi:10.1093/hmg/ddt157*

# Impaired viability of muscle precursor cells in muscular dystrophy with glycosylation defects and amelioration of its severe phenotype by limited gene expression

**Motoi Kanagawa[1], Chih-Chieh Yu[1,†], Chiyomi Ito[1,†], So-ichiro Fukada[2], Masako Hozoji-Inada[1], Tomoko Chiyo[3], Atsushi Kuga[1], Megumi Matsuo[1], Kanoko Sato[1], Masahiko Yamaguchi[2], Takahito Ito[2], Yoshihisa Ohtsuka[1], Yuki Katanosaka[4], Yuko Miyagoe-Suzuki[3], Keiji Naruse[4], Kazuhiro Kobayashi[1], Takashi Okada[3], Shin'ichi Takeda[3] and Tatsushi Toda[1,*]**

[1]Division of Neurology/Molecular Brain Science, Kobe University Graduate School of Medicine, Kobe 650-0017, Japan, [2]Laboratory of Molecular and Cellular Physiology, Graduate School of Pharmaceutical Sciences, Osaka University, Suita 565-0871, Japan, [3]Department of Molecular Therapy, National Institute of Neuroscience, National Center of Neurology and Psychiatry, Kodaira 187-8502, Japan and [4]Department of Cardiovascular Physiology, Graduate School of Medicine, Dentistry and Pharmaceutical Sciences, Okayama University, Okayama 700-8558, Japan

Received January 7, 2013; Revised March 3, 2013; Accepted April 2, 2013

**A group of muscular dystrophies, dystroglycanopathy is caused by abnormalities in post-translational modifications of dystroglycan (DG). To understand better the pathophysiological roles of DG modification and to establish effective clinical treatment for dystroglycanopathy, we here generated two distinct conditional knock-out (cKO) mice for *fukutin*, the first dystroglycanopathy gene identified for Fukuyama congenital muscular dystrophy. The first dystroglycanopathy model—myofiber-selective fukutin-cKO [muscle creatine kinase (MCK)-fukutin-cKO] mice—showed mild muscular dystrophy. Forced exercise experiments in presymptomatic MCK-fukutin-cKO mice revealed that myofiber membrane fragility triggered disease manifestation. The second dystroglycanopathy model—muscle precursor cell (MPC)-selective cKO (Myf5-fukutin-cKO) mice—exhibited more severe phenotypes of muscular dystrophy. Using an isolated MPC culture system, we demonstrated, for the first time, that defects in the fukutin-dependent modification of DG lead to impairment of MPC proliferation, differentiation and muscle regeneration. These results suggest that impaired MPC viability contributes to the pathology of dystroglycanopathy. Since our data suggested that frequent cycles of myofiber degeneration/regeneration accelerate substantial and/or functional loss of MPC, we expected that protection from disease-triggering myofiber degeneration provides therapeutic effects even in mouse models with MPC defects; therefore, we restored fukutin expression in myofibers. Adeno-associated virus (AAV)-mediated rescue of fukutin expression that was limited in myofibers successfully ameliorated the severe pathology even after disease progression. In addition, compared with other gene therapy studies, considerably low AAV titers were associated with therapeutic effects. Together, our findings indicated that fukutin-deficient dystroglycanopathy is a regeneration-defective disorder, and gene therapy is a feasible treatment for the wide range of dystroglycanopathy even after disease progression.**

*To whom correspondence should be addressed at: 7-5-1 Kusunoki-chou Chuo-ku, Kobe 650-0017, Japan. Tel: +81 783826287; Fax: +81 783826288; Email: toda@med.kobe-u.ac.jp
†These authors contributed equally to this work.

## INTRODUCTION

Dystroglycanopathy includes Walker–Warburg syndrome, muscle–eye–brain disease, Fukuyama congenital muscular dystrophy (FCMD) and several forms of congenital and limb–girdle muscular dystrophies (1). Dystroglycanopathy is indicated by a wide variety of clinical symptoms; the most severe end of the clinical spectrum is characterized by congenital muscular dystrophy with severe structural brain and eye abnormalities, whereas the mildest end presents in adult life with limb–girdle muscular dystrophy without brain or eye involvement (1). FCMD is the first dystroglycanopathy to be reported (2,3), and it is the second most common childhood muscular dystrophy in Japan. The founder mutation, a SINE-VNTR-*Alu* retrotransposon insertion in the 3′ noncoding region of *fukutin*, causes abnormal splicing that leads to the production of non-functional proteins in FCMD (4,5). FCMD is characterized by severe congenital muscular dystrophy, abnormal neuronal migration associated with mental retardation and epilepsy and, frequently, eye abnormalities. It often results in early death before the age of 20 (6). Several point mutations in *fukutin* have also been reported to be associated with dystroglycanopathy in Japan and other countries (7,8).

More than 10 genes [protein *O*-mannosyltransferase 1 (*POMT1*), protein *O*-mannosyltransferase 2 (*POMT2*), protein *O*-linked mannose β-1,2-*N*-acetylglucosaminyltransferase 1 (*POMGNT1*), *fukutin*, fukutin-related protein (*FKRP*), *LARGE*, dolichol-phosphate-mannose synthase (*DPM2* and *DPM3*), isoprenoid synthase domain containing (*ISPD*) gene, glycosyltransferase-like domain containing 2 (*GTDC2*) gene and β-1,3-*N*-acetylglucosaminyltransferase 1 (*B3GNT1*)], implicated in dystroglycanopathies, have been shown or expected to be involved in the glycosylation pathway of α-dystroglycan (α-DG) (1,9,10). POMGnT1 and the POMT1/2 complex possess glycosyltransferase activities and can directly synthesize *O*-mannosyl sugar chains on α-DG (11,12). Fukutin, FKRP and LARGE are involved in a novel phosphodiester-linked modification, namely, a post-phosphoryl modification, of *O*-mannose on α-DG (13,14). Recently, it has been shown that LARGE can act as a bifunctional glycosyltransferase with both xylosyltransferase and glucuronyltransferase activities (15). The DG gene *DAG1* encodes both α- and β-DG, which is post-translationally cleaved into the two subunits (16). α-DG is a highly glycosylated protein and serves as the receptor subunit for extracellular proteins such as laminins, perlecan, agrin, neurexin and pikachurin (9,17). *O*-mannosyl glycosylation and the post-phosphoryl modification are required for the ligand-binding activities of α-DG (3,13). Hypoglycosylation and reduced ligand-binding activity of α-DG are common characteristics of dystroglycanopathy. α-DG is anchored to the plasma membrane through non-covalent interactions with the transmembrane subunit β-DG. β-DG intracellularly interacts with dystrophin, whose mutations lead to Duchenne/Becker muscular dystrophy, and dystrophin, in turn, binds to actin filaments. This molecular linkage, created by laminin-DG-dystrophin-actin filaments, is thought to provide mechanical stability to the plasma membrane of the muscle fiber; thus, disruption of this linkage is considered a key pathological event in several forms of muscular dystrophy. In FCMD skeletal muscles, in addition to dystrophic muscular changes, there are certain characteristics such as intensive connective tissue infiltration and the presence of predominant small-sized fibers from the early infantile stage (6). Furthermore, aberrant neuromuscular junctions and delayed muscle fiber maturation have been implicated in the pathology of FCMD (18). FCMD also shows central nervous system involvement. Together, these data suggest that more complex and unknown physiological roles of α-DG modification underlie the skeletal muscle pathology of dystroglycanopathy.

Recent studies have identified new genes associated with dystroglycanopathy (19–21), and an increasing number of patients are being diagnosed with dystroglycanopathy worldwide. However, the pathogenesis of this condition is not fully understood, and no effective clinical treatment has been established. To understand the pathogenesis and establish a therapeutic strategy for dystroglycanopathy, we developed two distinct *fukutin* conditional knock-out (cKO) mice as models for dystroglycanopathy. In our study, investigation of presymptomatic fukutin-deficient mice provided direct evidence that fragility of the myofiber membrane triggers the pathogenesis of dystroglycanopathy. We also used an isolated muscle precursor cell (MPC) culture system to demonstrate, for the first time, that defects in the fukutin-dependent modification of DG lead to impairment of MPC proliferation, differentiation and muscle regeneration. We predicted that protection from disease-triggering myofiber degeneration would prevent substantial and/or functional loss of MPC, thereby providing therapeutic effects. Indeed, we demonstrate that restoration of fukutin expression in myofibers successfully ameliorates the severe pathology even after disease progression. These results indicate that gene therapy is a feasible treatment for dystroglycanopathy.

## RESULTS

### Generation and characterization of myofiber-selective fukutin cKO mice

To generate *fukutin*-cKO mice, flox fukutin mice (*fukutin*$^{lox/lox}$) were crossed with muscle creatine kinase (MCK)-Cre mice (22) or Myf5-Cre mice (23), which express the *Cre* gene with the help of the MCK promoter or Myf5 promoter, respectively (Supplementary Material, Fig. S1). The MCK promoter is active in differentiating and differentiated muscle cells (24), and MCK expression reaches maximum levels at post-natal day 10 and remains constantly high throughout life (25). First, we analyzed the MCK-fukutin-cKO mice at different time points. In the skeletal muscles of these mice, we confirmed dramatic reduction in the fukutin protein after the age of 4 weeks (Fig. 1A). Abnormal modification of α-DG is indicated by decreased molecular weight, loss of immunoreactivity against the monoclonal IIH6 antibody, which recognizes properly glycosylated α-DG (3), and decreased laminin-binding activity. Abnormally modified α-DG was predominant in MCK-fukutin-cKO mice aged >8 weeks (Fig. 1A). Loss of the post-phosphoryl modification was further confirmed by subjecting the protein to treatment with cold aqueous hydrofluoric (HF) acid, which cleaves phosphoester linkages, and to inorganic metal-affinity chromatography (IMAC), which captures monoester-linked phosphorylated compounds

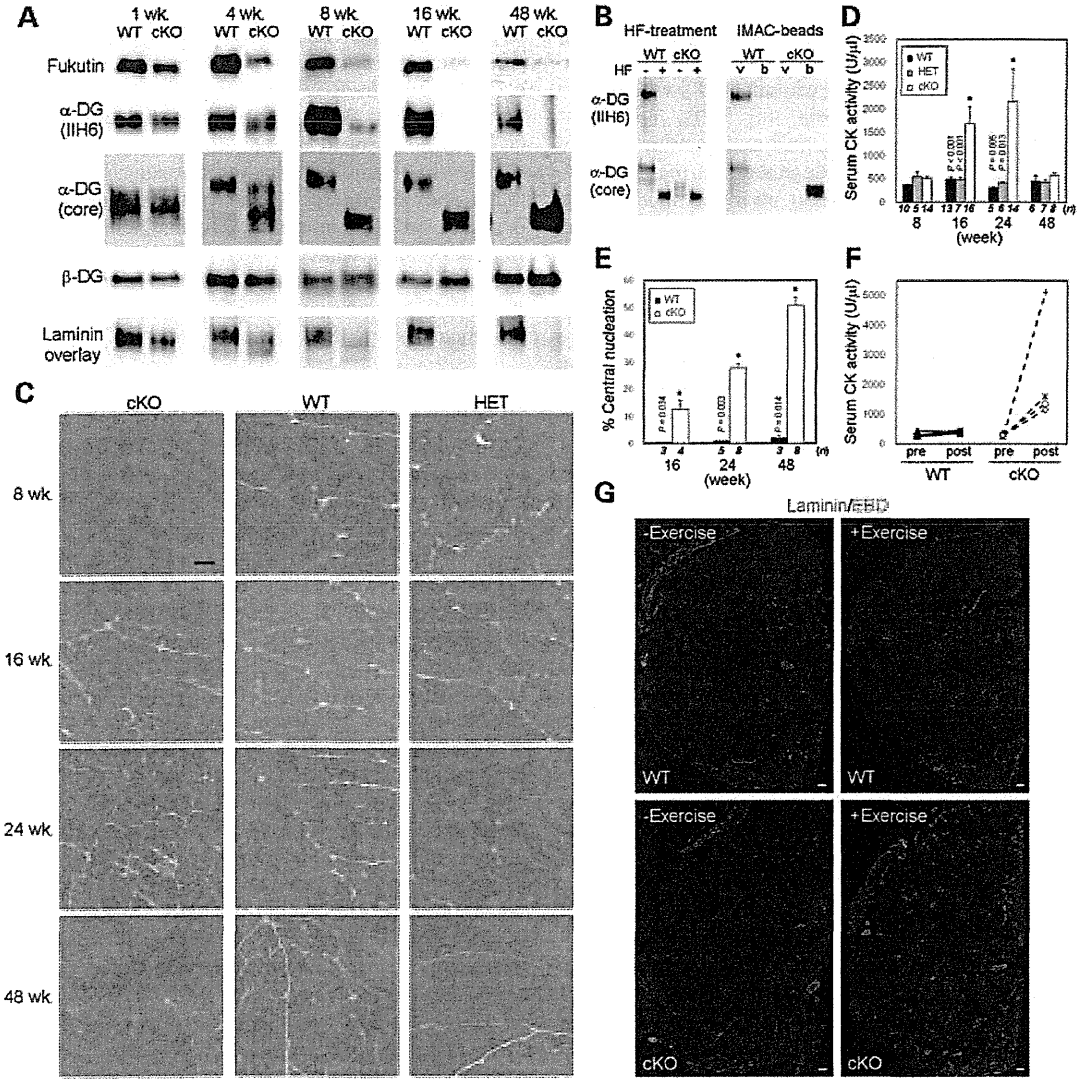


**Figure 1.** Pathological characterization of MCK-fukutin-cKO mice. (**A**) Western blot analysis of fukutin protein expression and α-DG modification in MCK-fukutin-cKO (cKO) and litter control WT skeletal muscles at different ages (1, 4, 8, 16 and 48 weeks). β-DG was used as a loading control. Laminin-binding activity of α-DG was examined by the laminin overlay assay. (**B**) Post-phosphoryl modification of α-DG from MCK-fukutin-cKO and control WT skeletal muscles. The absence of the post-phosphoryl modification was confirmed by HF treatment and IMAC-bead-binding assay. The void (v) and bound (b) fractions of the IMAC beads were analyzed by western blotting. (**C**) H&E staining of tibialis anterior muscles. Bar = 50 μm. (**D**) Serum CK activity and (**E**) proportion of myofibers with centrally located nuclei. Data shown are mean ± SEM for each group ($n$ is indicated in the graph). $^*P \leq 0.05$ for both cKO versus WT and cKO versus HET (D) and cKO versus WT (E) (Mann–Whitney $U$ test; $P$-values are indicated in the graph). (**F**) Serum CK activity before and after forced exercise. Serum CK levels of individual mice ($n = 4$ in each genotype) were measured before (pre) and after (post) exercise. (**G**) Uptake of Evans blue dye into myofibers after forced exercise. MCK-fukutin-cKO and control WT mice were subjected to forced exercise (+Exercise); subsequently, the muscle sections were stained with laminin (green) for individual fibers and merged with Evans blue dye (red). Mice not subjected to exercise were used as controls (−Exercise). Bar = 200 μm.

(13,14). The molecular weight of α-DG in the skeletal muscles of control (WT) mice was dramatically reduced after HF treatment, and α-DG did not bind to IMAC beads because the phosphodiester-linked modification was intact; in contrast, α-DG in the skeletal muscles of MCK-fukutin-cKO mice showed little sensitivity to HF and bound to IMAC beads (Fig. 1B), indicating incomplete post-phosphoryl modification. Immunofluorescence staining with an antibody against an α-DG core protein showed that α-DG localized to the sarcolemma of MCK-fukutin-cKO mice as seen in normal controls (Supplementary Material, Fig. S2A), which suggests that cellular trafficking of α-DG is little affected by fukutin deficiency. These results confirmed abnormal modification of α-DG in the skeletal muscles of MCK-fukutin-cKO mice.

Hematoxylin and eosin (H&E) staining revealed that 16-week-old MCK-fukutin-cKO mice showed signs of muscular dystrophy, such as myonecrosis and central nucleation (Fig. 1C). Serum creatine kinase (CK) activity in